DOT/FAA/TC-15/60

Federal Aviation Administration
William J. Hughes Technical Center
Aviation Research Division
Atlantic City International Airport
New Jersey 08405

Analysis Methods for the Management of Structural Damage With Structural Health Monitoring

October 2017

Final Report

U.S. Department of Transportation
Federal Aviation Administration

NOTICE

Technical Report Documentation Page

1. Report No.	2. Government Accession No.	3. Recipient's Catalog No.
DOT/FAA/TC-15/60		

4. Title and Subtitle	5. Report Date
ANALYSIS METHODS FOR THE MANAGEMENT OF STRUCTURAL DAMAGE WITH STRUCTURAL HEALTH MONITORING	October 2017
	6. Performing Organization Code

7. Author(s)	8. Performing Organization Report No.
Wu, Y.-T.[1] and Millwater, H.R.[2]	

9. Performing Organization Name and Address	10. Work Unit No. (TRAIS)
[1] Applied Research Associates, Inc., Raleigh, NC [2] Univ. of Texas, at San Antonio, TX	11. Contract or Grant No. FAA 07-G-018

12. Sponsoring Agency Name and Address	13. Type of Report and Period Covered
U.S. Department of Transportation Federal Aviation Administration FAA Central Regional Office 901 Locust St Kansas City, MO 64106	Technical report Sept. 2007 to Sept. 2010
	14. Sponsoring Agency Code ACE-113

15. Supplementary Notes

The FAA William J. Hughes Technical Center Aviation Research Division Technical Monitor was Sohrob Mottaghi.

16. Abstract

The objective of this project is to develop advanced efficient and accurate analysis methods and tools to support reliability or risk-based maintenance optimization (RBMO) of aircraft structural reliability by using monitored or inspected data in combination with damage tolerance (DT) physics-based models.

The progress in the adoption of the RBMO technology has been relatively stagnant because of the lack of integrated methodology and tools to address application issues, such as probabilistic model building and computationally efficiency and accuracy. This report presents an integrated, efficient, and versatile RBMO methodology built on a two-stage random simulation framework and features three tightly-integrated efficient methods: (1) a new adaptive reliability-based adaptive meta-modeling approach to establish an accurate and fast-running approximate DT model, (2) an existing adaptive stratified importance sampling method for computing probability-of-failure without inspection and to generate random failure samples, and (3) an existing recursive probability integration method for computing probability-of-failure with inspections and repairs. The integrated methodology, implemented in a software tool, is demonstrated using a fracture mechanics code with several random variables, a random probability of detection (POD), several repair qualities, and multiple inspections.

The basis of the DT approach is the recognition and modeling of initial flaws and the incorporation of inspection and repair/replacement to sustain structural reliability and safety. However, the drawback is the lack of data to build reliable probabilistic distributions, including the initial flaw size distribution, POD, and other fracture mechanics-related parameters. This report investigates the computational challenges and proposes an efficient computational strategy for updating probabilistic DT modeling assumptions using detected/monitored data. The proposed computational Bayesian framework is based on using crack (or other forms of measurable damage) growth and the PODs to create likelihood functions, has laid a foundation for incorporating damage detection results from multiple locations and times, including scheduled inspections and structural health monitoring for which the data are monitored continuously. The computational efficiency is achieved by the adoption of the Markov Chain Monte Carlo sampling method and the traditional response surface method to compute the crack size probability density functions . The approach is demonstrated using a fracture mechanics example.

17. Key Words	18. Distribution Statement
Bayesian updating, Damage tolerance, Fatigue, Fracture mechanics, Structural health monitoring, Structural reliability, Probabilistic methods, Reliability methods	This document is available to the U.S. public through the National Technical Information Service (NTIS), Springfield, Virginia 22161. This document is also available from the Federal Aviation Administration William J. Hughes Technical Center at actlibrary.tc.faa.gov..

19. Security Classif. (of this report)	20. Security Classif. (of this page)	21. No. of Pages	22. Price
Unclassified	Unclassified	52	

ACKNOWLEDGEMENTS

The FAA Technical Monitor for this project was Dr. Michael Shiao, who has contributed through significant technical review meeting discussions and by providing technical insights to the recursive probability integration method and its application to reliability-based maintenance optimization.

TABLE OF CONTENTS

LIST OF FIGURES

LIST OF TABLES

LIST OF SYMBOLS AND ACRONYMS

D	Detected/measured data, $D = (D_1, D_2, .. D_m)$
$F(D)$	CDF of D
$f(D)$	PDF of D
$g(X)$	Limit state function of X variables
$L(D\|\theta)$	Likelihood function
l	Number of parameters to be updated
N	Number of detected data
p_f	Probability of failure
t	Service time associated with D
θ	Distribution parameters to be updated
$q^-(\theta)$	Prior distribution of θ
$q^+(\theta\|D)$	Posterior distribution of θ
$g(\boldsymbol{X})$	Limit state or failure function of random variable vector $\boldsymbol{X}$
p_f	Probability-of-failure
p_f^{W0}	p_f without inspections
p_f^{W}	p_f with inspections
u	Standard normal variate (random variable)
$\Phi(.)$	CDF of standard normal RV
$\phi(.)$	PDF of standard normal RV
ASIS	Adaptive stratified importance sampling
CV	Cross-validation
CDF	Cumulative distribution function
DT	Damage tolerance
EIFS	Equivalent initial flaw size
FPA	Fast probability analyzer
MC	Monte Carlo
MCMC	Markov Chain Monte Carlo
NDI	Nondestructive inspection
PDF	Probability density function
PND	Probability of non-detection
POD	Probability of detection
POF	Probability-of failure
RAM	Reliability-based adaptive meta-modeling
RBMO	Risk- (reliability)-based maintenance optimization
RPI	Recursive Probability Integration for computing p_f with inspections and repairs
RV	Random variable
SHM	Structural health monitoring

EXECUTIVE SUMMARY

The objective of this research was to develop advanced, efficient, and accurate analysis methods and tools to support reliability- or risk-based maintenance optimization (RBMO) of aircraft structural reliability by using monitored or inspected data in combination with damage tolerance (DT) physics-based models. The research was motivated by the Federal Aviation Administration Rotorcraft Directorate's decision to accept the recommendations by the Technical Oversight Group for Aging Aircraft to use the DT method to implement DT requirements in Title 14 Code of Federal Regulations Part 29.571, Fatigue Evaluation of Rotorcraft Structures (Rotorcraft Working Group Report, 1999; 2001). The DT approach recognizes the existence of initial anomalies or flaws and incorporates inspection and repair/replacement as an important method for sustaining structural reliability and safety.

The project has two technology thrusts: (1) to advance RBMO methodology and (2) to address the uncertainty of the probabilistic input data. A practical and technically solid RBMO methodology, combined with inspection or monitoring data, is required for a successful application of the Bayesian probability theory for DT-based maintenance decision making.

Progress in the development of RBMO technology has been somewhat stagnant because of a lack of integrated methodologies and tools that address application issues, such as probabilistic model building and computational efficiency and accuracy. This report presents an integrated, efficient, and versatile RBMO methodology built on a two-stage, random simulation framework and features three tightly integrated efficient methods: (1) a new reliability-based adaptive meta-modeling (RAM) approach to establish an accurate and fast-running approximate DT model, (2) an existing adaptive stratified importance sampling method for computing probability-of-failure (POF) without inspection and generating random failure samples, and (3) an existing recursive probability integration method for computing POF with inspections and repairs. The integrated methodology, implemented in a software tool, is demonstrated using a fracture mechanics code with several random variables, a random probability of detection (POD), several repair qualities, and multiple inspections. The example has demonstrated that the RBDO methods have reached a matured state that is applicable to analyzing complex DT problems. In particular, the new RAM approach has displayed a unique ability to generate focused training data that matter most to the accuracy of POF ,and therefore, it is suitable for analyzing computationally time-demanding DT models.

The drawback of DT is the lack of initial data to build reliable probabilistic distributions, including the initial flaw size distribution, POD, and other fracture mechanics-related parameters. It is well known that the input uncertainty issue can be addressed by the Bayesian probability theory. However, the conventional approach requires that the analyst provide a likelihood function that is not DT-model-based and often is time independent. Such an assumption is too restrictive to handle data that cover a wide range of service time for which the likelihood function should be time dependent. Recognizing the constraint, the computational Bayesian framework developed for this project is based on using crack (or other forms of measurable damage) growth and the PODs to create likelihood functions. This approach is more suited for incorporating damage-detection results from multiple locations and times, including scheduled inspections and structural health monitoring for which the data are monitored continuously. In addition, the computational efficiency is achieved by the adoption of the Markov Chain Monte Carlo (MCMC) sampling method and the traditional response surface method to compute the crack size probability density

functions (PDF). The approach is demonstrated using a fracture mechanics example. It is encouraging to note that even with the poor priors (one or more standard deviations away from the true value), the results have shown significantly improved posterior PDF using 10 defects and further improvement using 20 defects.

1. INTRODUCTION

The objective of this project was to develop advanced, efficient, and accurate analysis methods and tools to support reliability or risk-based maintenance optimization (RBMO) of aircraft structural reliability by using monitored or inspected data in combination with damage tolerance (DT) physics-based models.

The project has two research thrusts: (1) to advance the RBMO methodology and (2) to address the uncertainty of the probabilistic input data. A practical and technically solid RBMO methodology, combined with inspecting or monitoring data, is required for a successful application of the Bayesian probability theory for DT-based maintenance decision making.

The DT approach complements structural health monitoring (SHM), which provides updated usage data and alarming information. DT provides SHM with the ability to forecast and update the risk prediction by using the information provided by either the sensors or by scheduled or unscheduled nondestructive investigations. For fatigue damage management, probabilistic DT analysis is one of the methods used to predict the risk and to characterize the uncertain damage state of structures associated with damage initiation, accumulation, inspection, detection, and other maintenance effects [1].

However, there are several issues in the DT approach that need to be addressed:

- Assumptions of initial flaw sizes and other uncertainties in the DT models
- Uncertainties of multiple nondestructive inspection (NDI) techniques in terms of probability of detection (POD) applied at the inspections
- Selection of inspection intervals
- Maintenance-induced damage
- Quality of replacements

To resolve the issues, previous and current research efforts sponsored by the Federal Aviation Administration have developed two complementary methodologies. The first is a reliability-based damage tolerance (RBDT) methodology [2], presented in section 2, and the second is the Bayesian updating methodology, presented in section 3.

The RBDT methodology is based on a framework illustrated in figure 1 that includes a wide range of uncertainties, including:

- Random or uncertain parameters in material (e.g., threshold of the stress intensity factor, modulus of elasticity)
- Defect or flaw parameters (including size, shape, location, and the frequency of occurrence)
- Loading, type of usage (with frequency of occurrence)
- Finite element model (including modeling error)
- Crack growth model (including modeling error)
- Maintenance (including inspection schedules, frequency of inspections, POD curves, and repair/replacement methods and effects)

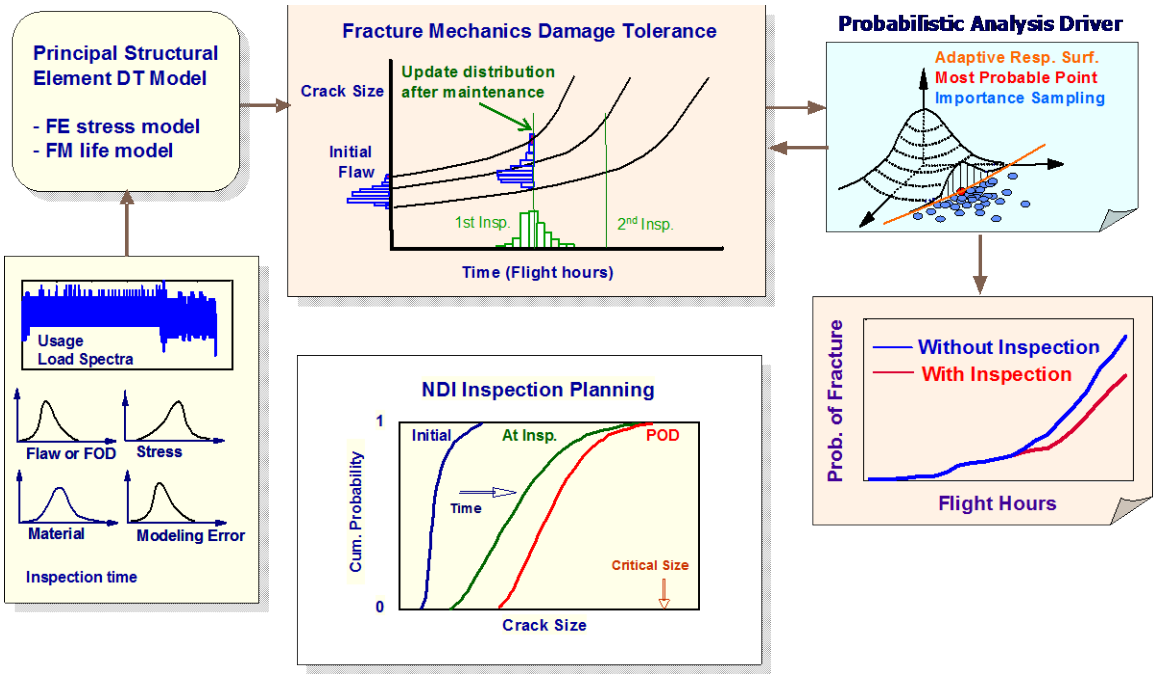

Figure 1. A reliability-based DT analysis framework (2004)

More recently, the RBMO methodology has been expanded to conduct automated RBMO as summarized in figure 2. The methodology has been implemented in a software tool, which includes a link to external DT codes, including NASGRO® Version 3.0. The RBMO methodology has the following key features [3]:

- Built on a two-stage sampling-based RBMO framework.
- Builds fast-running, approximate damage models using the reliability-based adaptive meta-modeling (RAM) method.
- Based on the RAM model, computes the probability of failure without inspections and generates random failure samples including damage-growth histories using the adaptive stratified importance sampling (ASIS) method.
- Retrieves the ASIS samples and applies the recursive probability integration (RPI) method to compute the probability of failure (POF) with inspections and repairs.
- Optimizes the maintenance plan by applying RPI to a set of user-selected or randomized inspection and repair strategies.

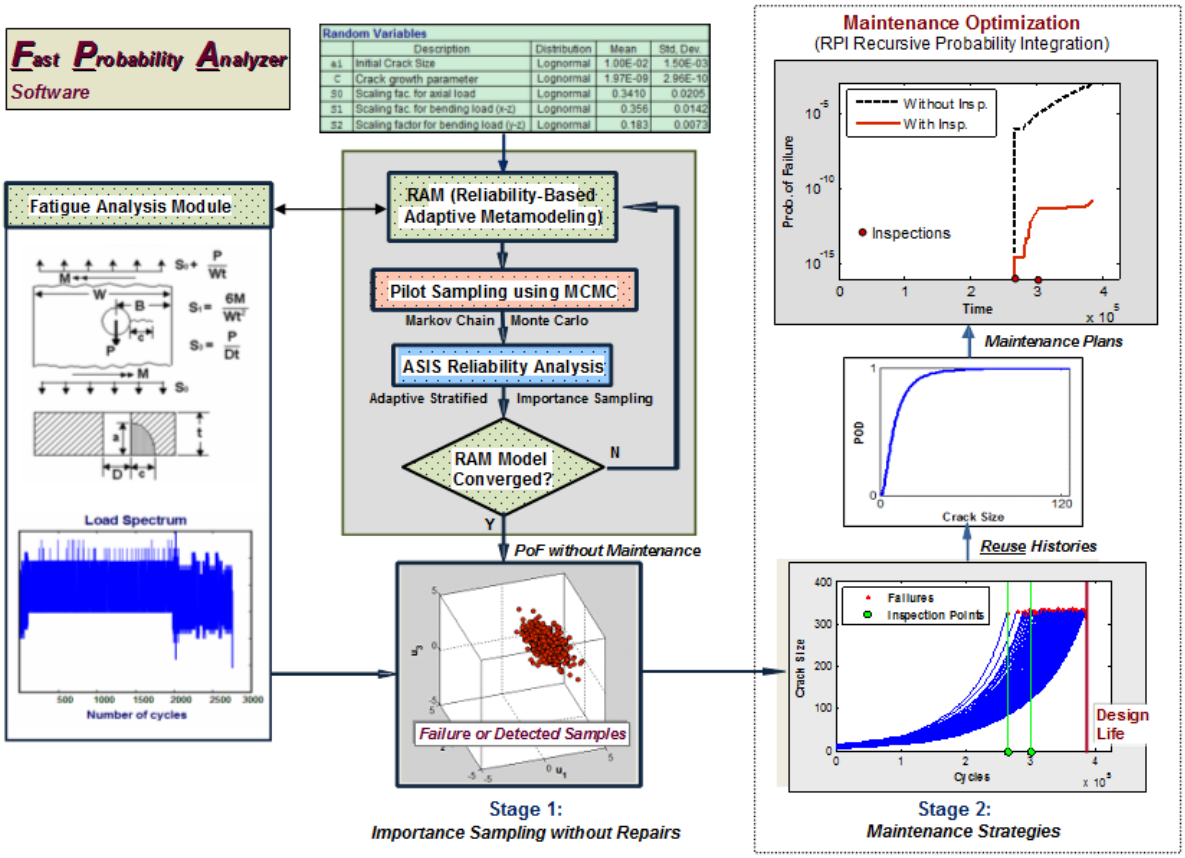

Figure 2. RBMO methodology

The effective use of RBMO requires well-characterized parameters; particularly, initial flaw size distribution and POD. Assuming a deterministic flaw size, as stated in MIL-A-83444 [4], is not realistic, and the reliability of the design cannot be quantified. Conversely, the initial flaw sizes are often too small to be detected by NDI tools, making it difficult to develop initial flaw-size probability distributions with confidence. A common approach to address this issue is to use grown and measurable defects at a later time (e.g., from a tear-down inspection) and apply fracture mechanics crack growth models to back-extrapolate the defect sizes to develop the equivalent initial flaw size (EIFS). However, it is well known that the EIFS derived under a specific condition is not suitable for different geometries or loading conditions. Even with the same geometries and loading conditions, the back-extrapolation process itself is non-deterministic because of the multiple sources of uncertainties involved in a typical crack growth process.

Characterizing the NDI capability using the POD is a well-accepted approach but can be impractical because POD is difficult to develop. The POD depends on many factors (e.g., devices, human factors, component geometries, defect shapes, sizes, locations, and orientations); therefore, it is difficult to acquire a sufficient number of components or specimens to develop the POD for different conditions, and it is more likely that the POD has a great deal of uncertainty.

To overcome the critical lack of data issues, this project applies Bayes' theorem to probabilistic DT models to update distributions. Though the application of Bayesian methods for fracture

mechanics has a long history [5], the application has primarily been limited to time-dependent likelihood functions. The formulation to include the time-dependent likelihood function is also available [6], but the implementation is difficult because of the computational issues involved in assessing the probability density function (PDF) of the detected defect size. Therefore, new efficient approaches are needed.

Section 2 presents new computational strategies to update uncertain parameters in probabilistic DT models using both detected data and missed indicators from different points in time. Reliability methods are used to develop the response surface of the cumulative distribution function (CDF) at a time of interest as a function of the crack size, and are conditioned on prior variables. The response surface is then used to facilitate the generation of random samples of the posterior PDF using the Markov Chain Monte Carlo (MCMC) method. The statistics of the random samples are retrieved to update the prior distribution, the reliability, and the plan for maintenance.

2. RELIABILITY- OR RISK-BASED MAINTENANCE OPTIMIZATION METHODOLOGY

2.1 INTRODUCTION

For economical and reliability/safety reasons, many structural systems rely on or can benefit significantly from inspection and repair to sustain reliability over the design life or extend the life beyond the original design. For example, aircraft are routinely inspected, including walk-around inspections for apparent damage and scheduled inspections to detect smaller or hidden flaws using specialized NDE devices. Oil and gas pipelines are regularly inspected using in-line inspection machines. When a significant defect or damage is detected and fixed, the strength will be changed, either repaired to the original or higher level, or reduced because of the repair methods and workmanship. To build a good reliability model, the post-repair strength should take into account the quality of repaired parts and workmanship. With a sound reliability model, the inspection schedules can be optimized subject to a reliability or risk constraint. Ideally, the timing of the inspections should be when the more dangerous defects can be detected with a high probability and before the POF has become unacceptable. The effects of inspections depend on several uncertain factors, including POD, damage growth rate, usage spectrum, and other random variables (RVs); therefore, a probability-based DT framework is appropriate.

At present, there are many structural reliability methods and software tools available for structural reliability analysis [7–9]. The methods include local approximation methods, global Monte Carlo (MC)-type methods, more sophisticated importance sampling and mixed methods (e.g., [4] and [10–18]), and methods that can be used for system reliability problems. Despite the progress, there are few generic approaches that are suitable for dealing with generic maintenance issues. Some exceptions are special applications, such as aircraft disks and wings [19–20], in which the number of RVs is fixed or the fracture mechanics model is tailored to certain geometries and materials. One of the reasons for the lack of progress is that, with the addition of inspections and repairs, the local approximation methods cannot be applied easily or at all, leaving only the random simulation methods that tend to be computationally intensive. Therefore, more efficient and general RBMO methods are still needed.

The foundation of the proposed sampling-based RBMO methodology is the two-stage maintenance simulation framework shown in figure 3 [2, 21]. The approach is built on the assumption that a

safe structure would not be degraded because of maintenance. Though special cases, such as poorly implemented maintenance practices, may cause the violation, the assumption is believed to be sound, especially for high-reliability products. Based on this assumption, only the fates of the potential failures need to be tracked. In the two-stage process, stage 1 generates candidate failure samples and computes the probability of failure assuming no inspections. Stage 2 takes the samples to assess the risk-reduction performances of various maintenance strategies.

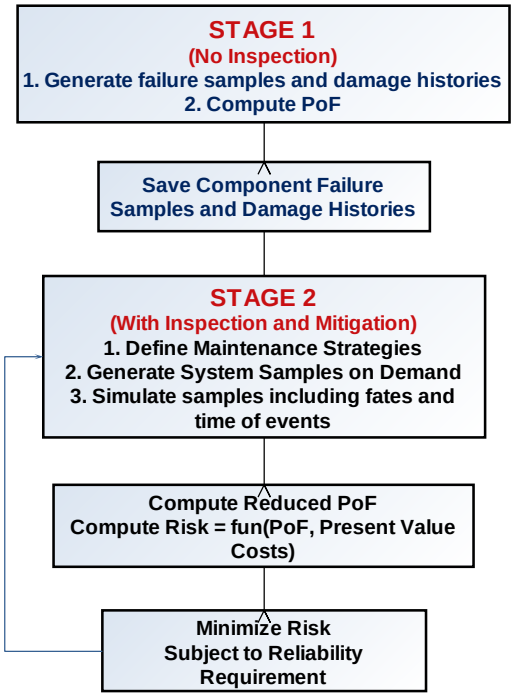

Figure 3. Two-stage RBMO framework

The two-stage framework was originally developed and demonstrated using applications with the additional assumption that the detected flaws would be perfectly repaired or that the chance of the repaired part failing in the future could be neglected [21]. The additional assumption ignores the possibility of poor repairs. Though the assumption led to a fast analysis and was valid for good quality repairs, it is nonconservative for potential poor repairs. In this report, this extra assumption has been removed and the repaired quality can be modeled using post-repair defect distributions.

Though the two-stage concept is straightforward, the challenges lie in the efficient computation of the POF, the generation of failure samples, and the computation of the POF with different degrees of repair quality. These challenges have been resolved using a combination of methods, including a new reliability-based adaptive metamodeling approach to build an accurate and fast-running approximate DT model, an ASIS method developed recently [22] for computing POF without inspections and generating random failure samples, and the RPI method [1] that has been incorporated to compute POF with inspections and repairs. The integrated RBMO methodology has been implemented in the Fast Probability Analyzer (FPA) software with an RBMO tool box. This report demonstrates the methodology by applying FPA/RBMO to a representative DT application example involving the use of NASGRO (Version 3.0) fracture mechanics code with several RVs, a random POD, several repair qualities, and multiple inspections.

2.2 UPDATED RELIABILITY- OR RISK-BASED MAINTENANCE OPTIMIZATION METHODOLOGY

The updated RBMO methodology includes the following key features:

- Built on a two-stage sampling-based RBMO framework.
- Builds fast-running approximate damage models using the RAM method. For simple analytical or other fast-running models, this method may be skipped.
- Computes the POF without inspections and generates random failure (or other conditioned) samples, including damage-growth histories using the ASIS method based on the RAM model.
- Retrieves the ASIS samples and applies the RPI method to compute POF with inspections and repairs.
- Optimizes the maintenance plan by applying RPI to a set of user-selected or randomized inspection and repair strategies.

The methodology was implemented in a MATLAB® software FPA with a probabilistic DT tool box, which includes a link to external DT codes. In this report, the NASGRO code, Version 3.0, was used to demonstrate the automated RBMO capability, as shown in figure 4. However, the methodology is not limited to any particular analysis code. The methods are summarized in sections 2.2.1–2.2.4.

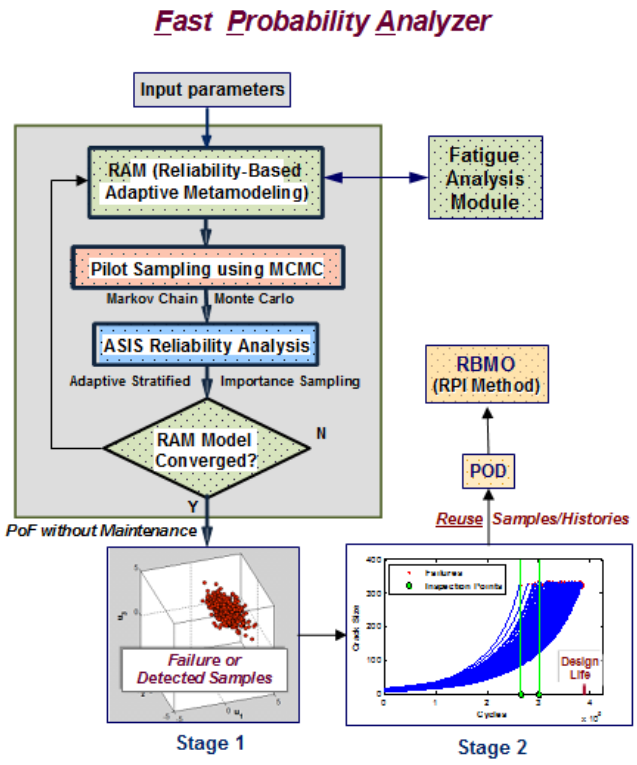

Figure 4. FPA software with RBMO tool box

2.2.1 Two-Stage Importance Sampling

The two-stage approach focuses on the samples of defects with failure potential, as illustrated in figure 5 using crack growth curves. Stage 1 computes POF without inspections, p_f^{W0}, and generates failure samples using the ASIS method described below, for the original and repaired defects. Stage 2 applies RPI for any number of maintenance strategies using the same stage 1 failure samples. If failure samples can be generated efficiently, the approach is much faster than the standard MC methods.

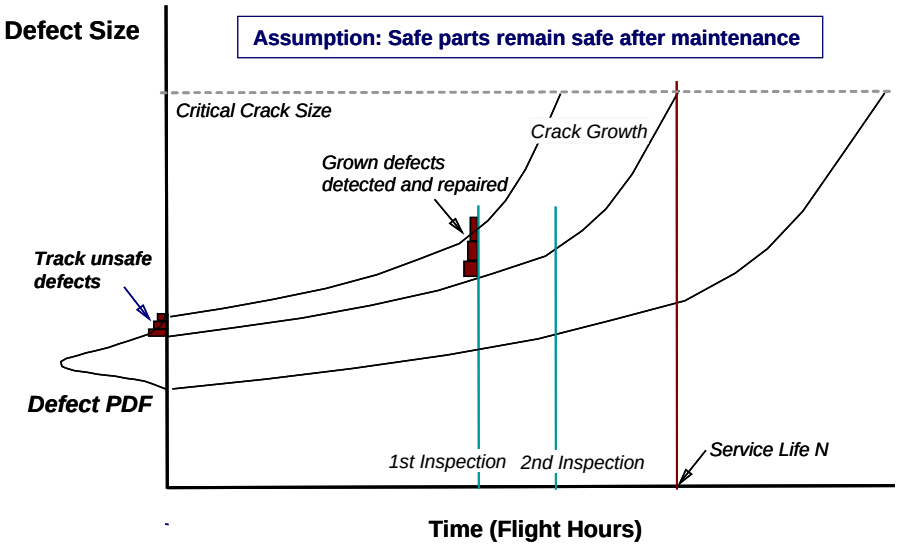

Figure 5. Two-stage approach focus on potential failure samples

2.2.2 Reliability-Based Adaptive Meta-Modeling

The computation of POF in stage 1 may be time consuming if each failure analysis takes significant time. To make the RBMO analysis faster, the RAM method has been developed. The uniqueness of the RAM approach is its ability to generate training data that matter most to the accuracy of POF. As a result, a relatively small amount of training data is usually required. Currently, the core of the RAM is a special version of the kriging method, but other meta-modeling methods, such as moving least squares, may also be appropriate.

A kriging model is commonly expressed as:

$$Y(\boldsymbol{x}) = f^T(\boldsymbol{x})\beta + Z(\boldsymbol{x}) \tag{1}$$

where $\boldsymbol{x}$ represents the interpolation points, $Y(\boldsymbol{x})$ is the sum of a linear regression model $f^T(\boldsymbol{x})\beta$, $Z(\boldsymbol{x})$ is a random process, $f(\boldsymbol{x}) = [f_1(\boldsymbol{x}), \dots, f_k(\boldsymbol{x})]^T$, and $\beta = [\beta_1, \dots, \beta_k]^T$. Typically, $Z(\boldsymbol{x})$ is assumed to have zero mean and a covariance function defined as:

$$\mathrm{COV}(\boldsymbol{x}_i, \boldsymbol{x}_j) = \sigma^2 R(\boldsymbol{x}_i, \boldsymbol{x}_j) \tag{2}$$

where σ is the standard deviation of $Z(\boldsymbol{x})$, and $R(\boldsymbol{x}_i, \boldsymbol{x}_j)$ is the correlation function. A well-adopted R function is the exponential model:

$$R(x_i, x_j) = R(d_{ij}, \theta) = e^{-\theta {d_{ij}}^2} \tag{3}$$

where d_{ij} is the distance between two points $\boldsymbol{x}_i$ and $\boldsymbol{x}_j$, and θ is a parameter to be estimated. Given R, the estimators of β are:

$$\hat{\beta} = (F^T R^{-1} F)^{-1} F^T R^{-1} y \tag{4}$$

where, for certain experimental design points with N points, $S = \{s_1, \dots, s_N\}$ and $F = [f(s_1, \dots, f(s_N)]^T$. The best linear unbiased prediction (BLUE) of the response at a prediction point $\boldsymbol{x}_0$ is [23 and 24]:

$$\hat{y}(\boldsymbol{x}_0) = f^T(\boldsymbol{x}_0)\hat{\beta} + r^T(\boldsymbol{x}_0)\hat{\alpha} \tag{5}$$

where $r^T(\boldsymbol{x}_0) = [R(\boldsymbol{x}_0, \boldsymbol{x}_1)\ R(\boldsymbol{x}_0, \boldsymbol{x}_2) \dots R(\boldsymbol{x}_0, \boldsymbol{x}_N)]$ and:

$$\hat{\alpha} = R^{-1}(y - F\hat{\beta}) \tag{6}$$

A well-used approach to estimate θ is cross-validation (CV) [25]. In the "leave one out" approach, θ is selected to minimize the sum of squared errors (SSE):

$$SSE(\theta) = \sum_{i=1}^{N} [\hat{Y}_{-i}(\boldsymbol{x}_i|\theta) - Y(\boldsymbol{x}_i)]^2 \tag{7}$$

where, $\hat{Y}_{-i}(x_i|\theta)$, for $i = 1{:}N$, is the prediction at $\boldsymbol{x}_i$ using the $\boldsymbol{x}_i$-excluded $(N - 1)$ points to build the predictor. Similarly, the CV can be designed to "leave n out," where $n > 1$.

Like any other known interpolator or a regression-type predictor, the accuracy of the prediction usually cannot be guaranteed or controlled. In general, the prediction errors are governed by the behavior of the response function and the distances between the fitting points. For reliability analysis, the required number of fitting points depends on the behavior of the response function and cannot be predetermined. In general, the nonlinear behavior of the response function cannot be easily managed, other than by variable transformations in certain special cases. A more feasible approach to reduce fitting errors is to use more fitting points or to assign more weights in the region of importance. For a reliability analysis that is governed by a fail-safe method, a good predictor should closely preserve the sign of the g function. If the sign of g remains the same in the region of high POF (i.e., there is a small probability of misclassification), it is acceptable, for the purposes of computing the p_f, to have large fitting errors. The optimal allocations of fitting points should be based on minimizing misclassifications in the region(s) of high POF.

These considerations have motivated the development of the new approach shown in figure 6. The approach consists of four steps:

1. The initial fitting points are set using the traditional design of experiments approach.

2. The number of fitting points are adaptively increased in the failure region (defined by the previous kriging model) with samples generated randomly according to the joint density function.
3. CV is applied to build the kriging models and check the fitting errors. Based on the magnitude of g, more weights are added to the points closer to $g = 0$ to provide a better reliability prediction. At this stage, the convergence criterion is based on the sum of residuals.
4. After the initial convergence, more points are added in increments to update the CV-based kriging model. The reliability-based convergence criterion is based on cumulative average of POF.

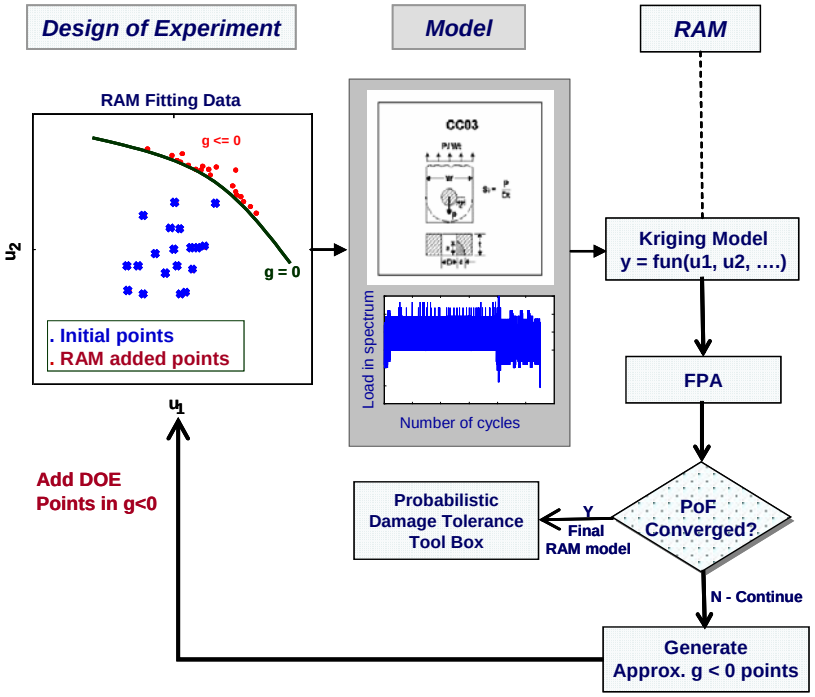

Figure 6. RAM

The ASIS reliability analysis is preceded by the MCMC sampling that generates pilot samples in the failure region. The Metropolis-Hastings algorithm was the preferred method for generating MCMC in the transformed, standardized normal space, $\boldsymbol{u}$. The Metropolis-Hastings algorithm can be summarized as follows:

1. Find a starting point, $\boldsymbol{u}_0$, in $g(\boldsymbol{u}) \leq 0$ by random search or other search methods.
2. Generate a candidate point, $\boldsymbol{v}$, using a conditional density $q(\boldsymbol{v}|\boldsymbol{u})$.

3. Take

$$\begin{aligned} \boldsymbol{u}_{\text{Next}} &= \boldsymbol{v} \text{ with probability } r(\boldsymbol{u},\boldsymbol{v}) \\ &= \boldsymbol{u} \text{ with probability } 1\text{-}r(\boldsymbol{u},\boldsymbol{v}) \end{aligned} \quad (8)$$

where

$$r(\boldsymbol{u},\boldsymbol{v}) = \min\left\{\frac{\phi(\boldsymbol{v})}{\phi(\boldsymbol{u})}\,\frac{q(\boldsymbol{u}|\boldsymbol{v})}{q(\boldsymbol{v}|\boldsymbol{u})}, 1\right\}$$

4. Repeat steps 2 and 3 as needed.

More details on the MCMC method are available in references 14, 26, and 27.

Figure 7 shows an MCMC example for which a starting point was found by a random search procedure. A burn-in period may be needed before keeping the MCMC samples.

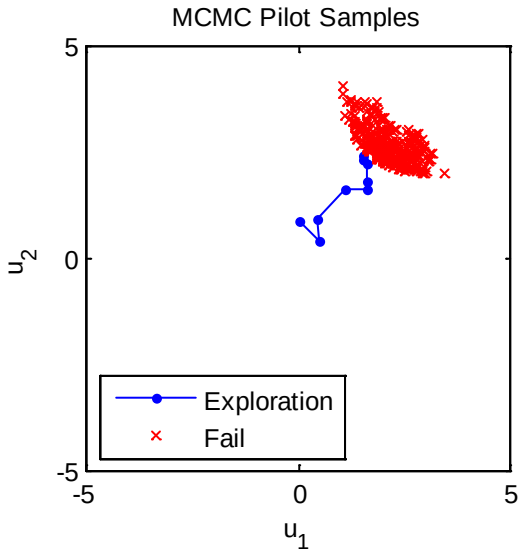

Figure 7. MCMC example

By the nature of a Markov Chain, the sequence of samples is correlated and the quality of the random samples is inferior to MC. Consequently, a larger number of samples is usually needed to achieve convergence. The MCMC algorithm itself does not directly provide an answer to the p_f, but the samples can be used as a foundation to supplement other methods, such as generating an approximate kernel density estimator as the importance-sampling density function [28] or being used in a subset simulation method [14] to compute POF. ASIS uses the MCMC samples to approximately envelop the failure region for importance sampling. As demonstrated by the example below, provided that MCMC is successful (i.e., not missing significant failure regions), ASIS can monitor and control the convergence of POF using a relatively small number of additional samples.

The ASIS method balances efficiency and accuracy by optimally distributing samples to stratified (i.e., divided) regions to minimize the variance of the POF sampling estimate. The concept is shown in figure 8 and a summary is given below.

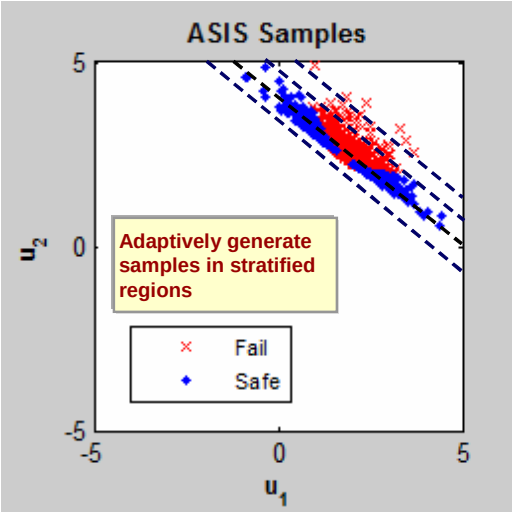

Figure 8**. Concept of ASIS**

The failure region is divided into *m* divisions. The POF is the sum of the *m* regional probabilities:

$$p_f = \sum_{j=1}^{m} A_j p_j \tag{9}$$

where A_j is the probability of region j and p_f denotes the POF. Let k_j be the number of samples in region j where the conditional POF is p_j and the reliability is q_j. The sampling estimates of p_j are approximated by binomial distributions. For a total number of samples, K, the optimal k_j are found by minimizing the variance of p_f , $\boldsymbol{\sigma_{P_f}}$ in equation 10:

$$\begin{aligned} &\text{Min. } H = \sigma_{P_f}^2 = \sum_{j=1}^{m} A_j^2 \frac{p_j q_j}{k_j} \\ &\text{Subject to: } K = \sum_{j=1}^{m} k_j \end{aligned} \tag{10}$$

Using the method of Lagrange multipliers, the sample sizes in the divisions can be derived [22]:

$$k_j = K\frac{A_j\sqrt{p_j q_j}}{\sum A_j\sqrt{p_j q_j}} \tag{11}$$

which, after substituting into equation 10, leads to:

$$\sigma_{p_f} = \frac{\sum A_j\sqrt{p_j q_j}}{\sqrt{K}} \tag{12}$$

By approximating the POF, p_f, as a normally distributed variable, the sampling error is:

$$\frac{\gamma(\%)}{100} = \frac{\varepsilon}{p_f} = \frac{z\sigma_{p_f}}{p_f} = \frac{-\Phi^{-1}(\alpha/2)\sigma_{p_f}}{p_f} \tag{13}$$

where z is the standardized normal variate and α is the risk. By substituting equation 13 into equation 12, the total number of samples becomes:

$$K = \left(100\frac{-\Phi^{-1}[(1-\mathrm{CL}(\%))/2]}{\gamma(\%)}\frac{\sum A_j\sqrt{p_j q_j}}{p_f}\right)^2 \tag{14}$$

where $\mathrm{CL} = 1-\alpha$ is the confidence level. The relative error, γ, is the target error at a specified CL.

The ASIS procedure consists of the following key steps:

1. Generate a sufficient number of MCMC samples.
2. Identify a sampling region that covers all or nearly all the samples.
3. Divide the sampling region using a design (e.g., using hyper-planes). Adjust the number of divisions to achieve optimal efficiency.
4. Adaptively increase k_j to update p_j and p_f to achieve convergence.
5. Use the converged p_j to generate proportionally random samples in A_j.

Although requiring additional samples, the quality of the ASIS-produced samples is better than MCMC and has been found to be more suitable for the stage 2 analysis. Figure 9 illustrates the roles of the two methods and visually compares the qualities of the samples.

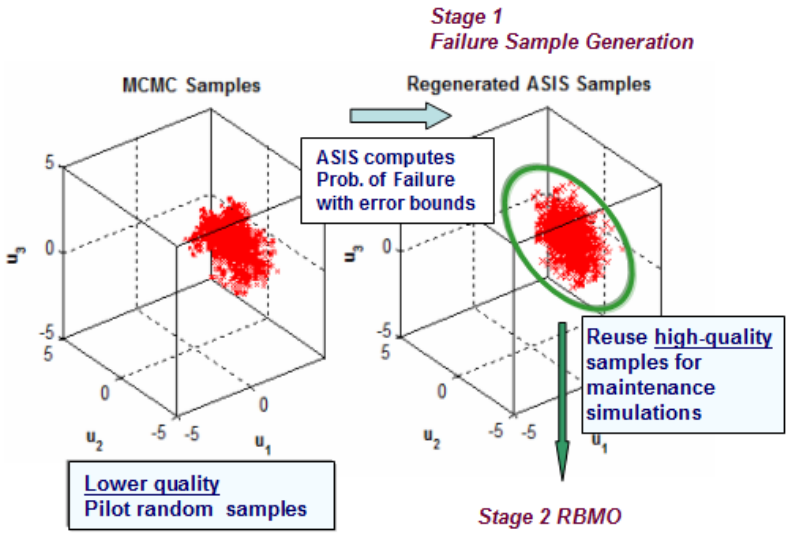

Figure 9. The roles of MCMC and ASIS

Note that the ASIS samples for RBMO can be generated using the RAM model, but the crack growth histories must be created using the original NASGRO model. In figure 9, the creation of the RAM model required 63 NASGRO runs, and an additional 1000 runs were executed to create the crack growth histories. The same process should be applied to each repair distribution.

2.2.3 Recursive Probability Integration

There are two outcomes from each inspection: (1) detected with POD or (2) missed with probability of non-detection (PND). A detected structural part is assumed to have been removed, replaced, or repaired using the original or a repair distribution. If missed, the damage will continue to grow until the next inspection or until the structure has failed. Figure 10 shows an event tree for an example with two inspections in which the branches of the events are identified by $Br(k, j_k, k)$. Each branched probability event consists of all possible events after the i^{th} inspection in the j^{th} simulation of MC simulations (denoted as j_k), starting at the k^{th} inspection (MCS(k)), where i = 1 to *2* and k = 0 to *2*. For each k *in* $Br(k, j_k, k)$, $i = k + 1$ to *2*. Also in the figure, FP(k), the k^{th} full path represents a probability event consisting of complete fatigue paths of an MCS considering subsequent inspections starting at the k^{th} inspection.

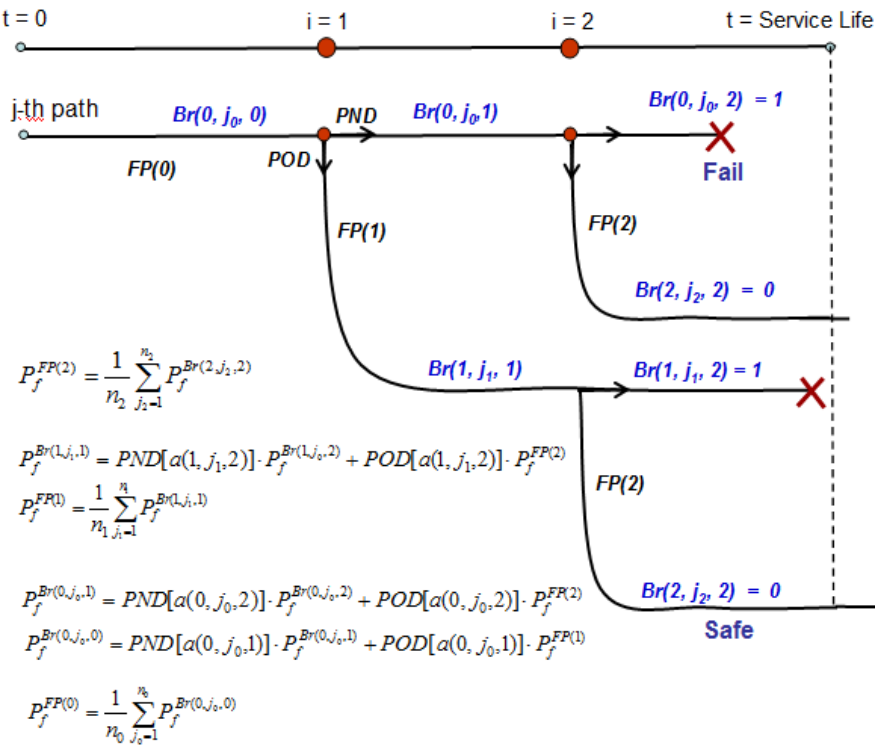

Figure 10. RPI for two inspections (only one j[th] realization is drawn for each MCS(k))

The number of the branched events will increase in the order of 2^m, where m is the number of inspections, and it will eventually become difficult to track and simulate each repair. Although the inspections and repairs can be simulated using standard random simulation methods, the implementation is tedious with the exception of a few inspections. In addition, using random simulations for detections will add variability to the POF with inspections, p_f^W, result. The RPI method simplifies the problem by using a concise formulation to manage any number of inspections and can significantly reduce the variance of p_f^W because the detection events are treated analytically rather than simulated randomly.

The RPI approach can be summarized in equations 15–17 [1].

$$p_f^{Full\ Path\ k} = \frac{1}{n_k}\sum_{j_k=1}^{n_k} p_f^{Br(k,j_k,k)} \qquad \text{where } k = m \text{ to } 0 \tag{15}$$

where n_k is the number of simulations in MCS(k); j_k represents the j^{th} simulation in the MCS (k). The "Full-Path k" in equation 15 is a complete sampling-based fatigue path for the original defect distribution (k = 0) and each repair distribution (k = 1 to m). The POF for the full paths is computed in reverse order, from $k = m$ to 0. For each sample j within an MC or ASIS simulation, the POF at the branches is computed, also in reverse order, using the following recursive equation:

$$p_f^{Br(k,j_k,i)} = PND(a(k,j_k,i+1)) \cdot p_f^{Br(k,j_k,i+1)} + POD(a(k,j_k,i+1)) \cdot p_f^{Full\ Path\ (i+1)} \quad (16)$$

where $i = m - 1$ to k.

where $a(k, i + 1)$ is the defect size at inspection $(i + 1)$ based on MC or ASIS simulations starting at inspection k. An example of equation 16 is provided in figure 10 for two inspections. By substituting the results from equation 16 into equation 15, the reverse roll-up of the branch probabilities lead to the final solution:

$$p_f^W = p_f^{Full\ Path\ 0} \quad (7)$$

Theoretically, m+1 sets of MC or ASIS samples are needed starting at time zero and after each m inspection. In practice, the types of repair distributions may be limited to a few; therefore, only a few sets of ASIS or MC failure samples are expected for RBMO.

2.2.4 Inspection Optimization

Inspection schedules are ordered, and the orders must be kept during optimization. Local minimums may also exist. Therefore, the traditional gradient-based optimizer may not be appropriate for RBMO applications. Instead, a simple random-search optimizer has been devised. In this approach, the service time is discretized and a large number of inspection plans are selected randomly. By applying RPI to all the inspection plans, the resulting p_f^W are ranked to identify the best plan. The method is reliable and the computational time is not a significant issue because stage 2 analysis is a relatively fast process.

2.3 DEMONSTRATION EXAMPLE

2.3.1 Damange Tolerance Model and Input Random Variables

The demonstration example was selected to represent a probabilistic DT problem typically found in aircraft or other structures with crack-growth issues. The data, including the input RVs, load spectrum, and POD, represent a typical structural part that is subjected to variable amplitude loads and would typically require a fatigue fracture code to compute crack-growth histories and lives. Note that the ASIS efficiency is insensitive to the probability level and both ASIS and RPI can compute POF to the level of 1.e-20, even though there is no practical meaning when POF is less than 1.e-08 or even 1.e-06. Nevertheless, the mathematical or "notional" p_f may be useful for comparing different strategies in a planning stage.

The defect of the structure to be analyzed is modeled as a corner crack (CC01) in NASGOR, as shown in figure 11. The RVs are listed in table 1. The service life is 386,000 cycles.

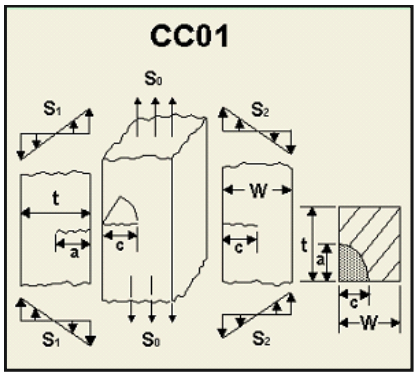

Figure 11. Corner crack model in NASGRO (Version 3.0)

Table 1. RVs for the CC01 model

Variable	Description	Distribution	Mean	Std, Dev
X (1) = ai	Initial Crack Size (in)	Lognormal	0.01	0.0015
X (2) = C	Crack growth parameter	Lognormal	1.97E-09	2.95E-10
X (3) = S0	Scaling factor for axial load	Lognormal	0.341	0.0205
X (4) = S1	Scaling factor for bending load (x-z)	Lognormal	0.356	0.0142
X (5) = S2	Scaling factor for bending load (y-z)	Lognormal	0.183	0.0073

2.3.2 Probabililty of Detection

The POD, plotted in figure 12, is modeled using the lognormal CDF curve with a mean of 3.15 mil and a standard deviation of 0.45 mil.

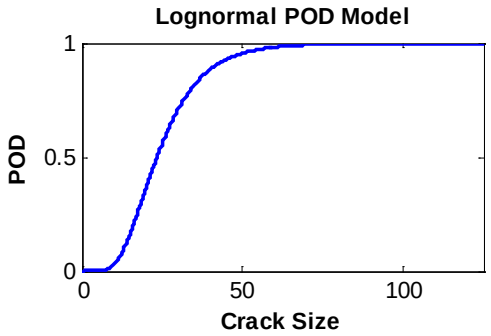

Figure 12. POD model (mils)

2.3.3 Reliability-Based Adaptive Meta-Modeling

Using the RAM approach, 63 fitting points were generated to achieve p_f convergence with a target error of 5% at 99% confidence. The goodness-of-fit of the RAM model is presented in figure 13 where *y* is the fracture life. The RAM analysis started with 20 randomly generated points that were,

as expected, all safe samples (i.e., lives > 380,000 cycles). The final 63 points included 24 failure samples.

The overall fitness of the RAM model was further validated using 100 independently generated random points. The validation result is shown in figure 14, which indicates that relatively larger errors are observed, as expected, for points further away from $g = 0$. However, the signs of g remain the same; therefore, the errors would not affect the accuracy of POF.

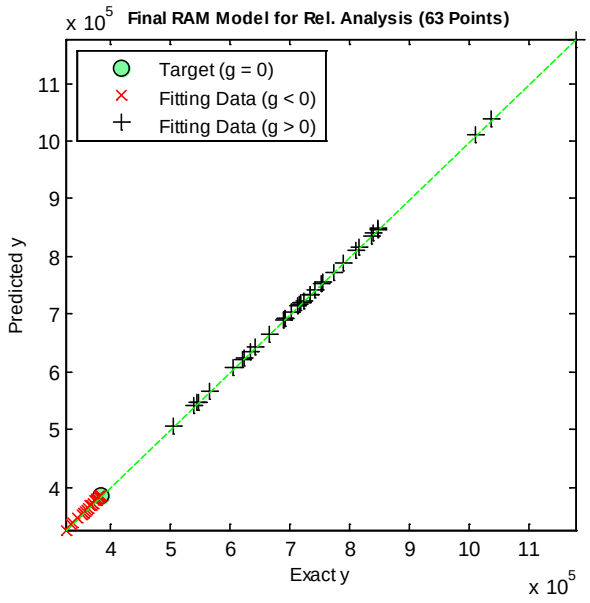

Figure 13. Goodness-of-fit of the RAM model

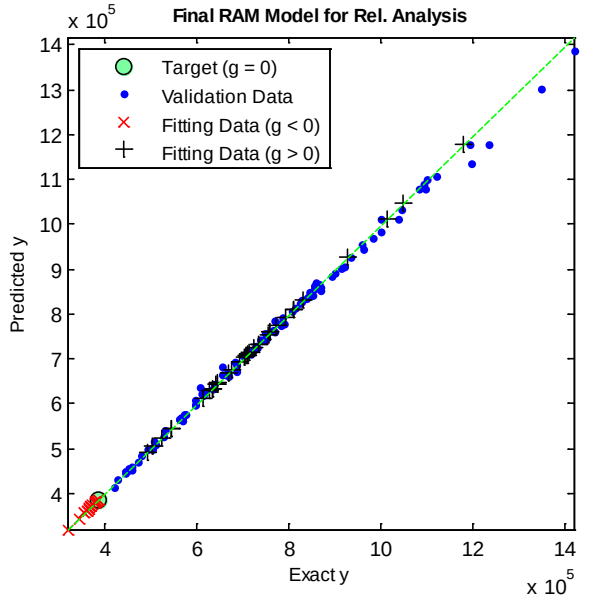

Figure 14. RAM validation (100 independent random validation points)

Figure 15 shows the p_f convergence plot for the RAM models using 47 to 63 points with an increment of 2 points. The cumulative average of p_f appears to converge rapidly. The converged p_f was 9.782e-04 with a preset 5% target error. Figure 16 shows the convergence history of the ASIS analysis using the final RAM model. Based on 2000 pilot MCMC samples, the convergence of the ASIS analysis was apparent after 500 ASIS samples. An independent first-order reliability method (FORM) analysis [13, 16, 17] resulted in a p_f of 0.00102, which suggests that the limit state is approximately linear in the transformed standard normal space. The FORM analysis can sometimes produce large errors [22] for highly nonlinear functions and is used here only as a reference.

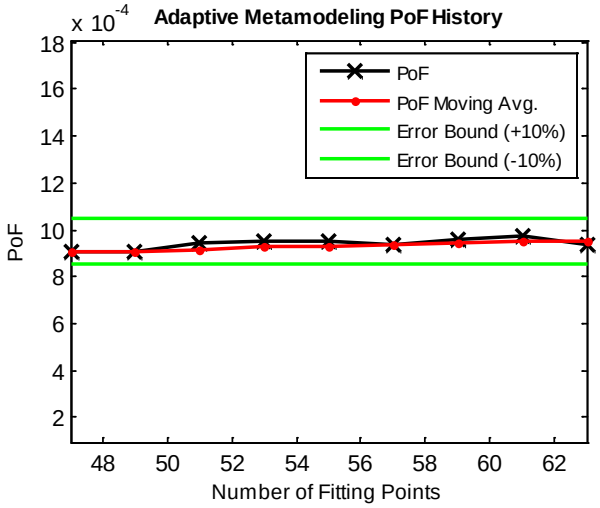

Figure 15. POF convergence using the RAM models

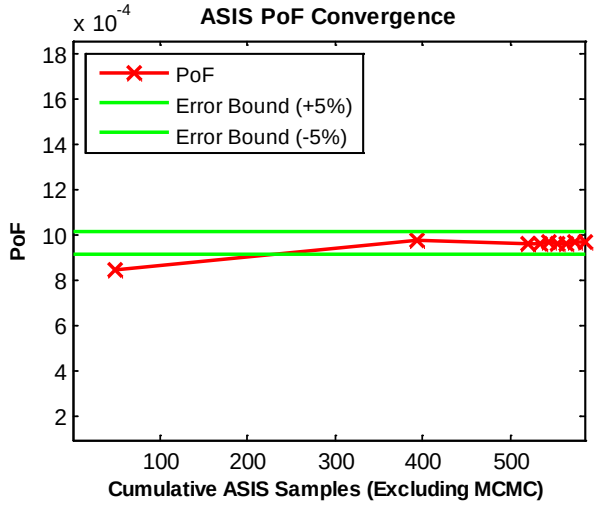

Figure 16. ASIS POF convergence using the final RAM model

2.3.4 Generation of Importance Samples Using Adaptive Stratified Importance Sampling

From the original initial flaw size distribution defined in table 1, 1000 failure samples were generated using the ASIS method. The equivalent number of MC samples is 1000/9.782e-04 = 1.02e+06. The corresponding 1000 crack growth curves, plotted in figure 17, were saved for Stage 2 RBMO. The figure illustrates that the crack size has grown from an initial mean value of 0.01 inches to approximately 0.18 inches at the time of the first inspection.

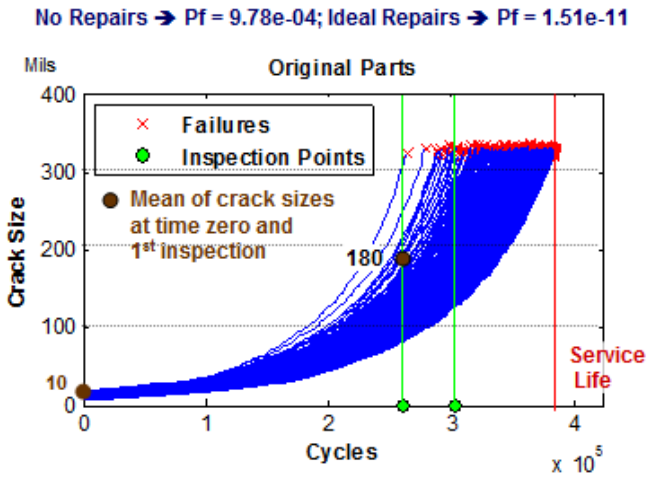

Figure 17**. 1000 crack growth curves for RBMO (inspections at 261370 and 302910 cycles)**

2.3.5 Post-Repair Defect Size Distributions

One important capability in RBMO is the ability to address different quality levels of repair. To address the issue in a practical manner, the quality level is defined here by choosing several repair size distributions associated with selected inspection time. For the demonstration example, two classes of repair are considered:

1. Ideal repair—After the repair, the defect is so small that there is essentially zero probability of failure for the remaining service life.
2. Regular repair—A repair or replacement for which the defect size is reduced (more probable) or increased (less likely).

Figures 18–20 illustrate three models of regular repairs with high (Q1), medium (Q2), and low (Q3) qualities, respectively. To simplify the calculations, the post-repair defect size distributions were defined at t_{Repair} = 261,370 cycles chosen based on the first inspection time using ideal repair.

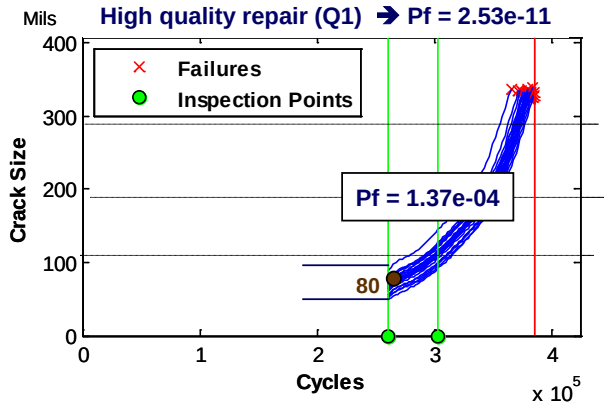

Figure 18. High-quality repair distribution

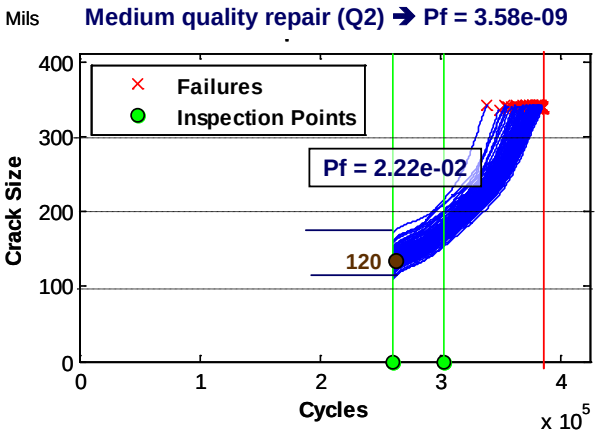

Figure 19. Medium-quality repair distribution

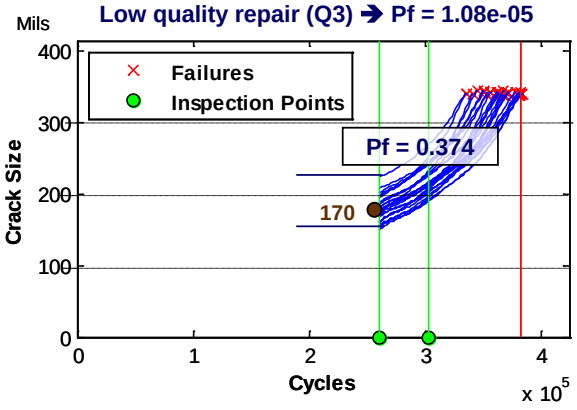

Figure 20. Low-quality repair distribution

By comparing figures 18–20 with figure 17, it can be seen that at t_{Repair} the medians of the three repair distributions are all smaller than the original median and the variability of the repaired defect sizes are significantly lower than the original. Therefore, the original largest defects which are near the critical size will be replaced by smaller defects so that there will be no imminent failure., In this study, we further assumed that the post-repair defect using the above distributions had escaped the inspection, to investigate a situation associated with a poor maintenance condition. In practice, the repair distribution should be modified using the POD. If the modified distributions were used in the subsequent analyses, the p_f^W's would be smaller.

By re-initializing service time from t_{Repair}, the remaining service life is 386000 - t_{Repair} = 124630 cycles and the conditional POFs are 1.37e-04 (Q1), 2.22e-02 (Q2), and 0.374 (Q3). Each conditional POF was calculated by ASIS and the corresponding stage 1 failure samples were generated and saved. During the stage 2 analyses, the crack growth curves were shifted based on selected inspection times: (1). If the inspection time was greater than t_{Repair}, the saved lives would be increased by t_{Repair}. (2). If the inspection time was smaller than t_{Repair}, the crack growth curves would be extended to the left (to t_{Insp}) by using the same defect size distribution at t_{Repair}. The above adjustments were made to avoid the need to create stage 2 samples for every given inspection. If more accuracy is needed, stage 1 analysis can be carried out for various t_{Repair}.

Using RPI, the POFs with two inspections (p_f^W) were 2.53e-11 (Q1), 3.58e-09 (Q2), and 1.05e-05 (Q3), which suggests that the conditional p_f's are correlated with p_f^W's. These results imply that the quality of the repair can be ranked by the conditional POF**.**

Using the ideal repair, the POF was 1.51e-11, which suggests that the quality of Q1 repair is at the same level as the ideal repair. To simplify, the best (ideal), the fair (regular–Q2), and the worst (regular–Q3) repairs are compared.

2.3.6 Inspection Optimization

The goal of the optimization was to find the best timing for 0 to 4 inspections for three repair cases. In this study, 1000 failure samples were used. The RPI results for 1 to 4 inspections are presented in figure 21. Two conclusions can be drawn: (1) POFs are significantly reduced by a small number of inspections for all three cases, and (2) for each regular repair with at least one inspection, the decrease of p_f^W by adding one inspection is more than the differences of p_f^W between the ideal and the regular repair. This implies that the decrease in repair quality, even in the worst (Q3) repair, can be compensated by adding one repair. In general, a plot like figure 21 should be useful for a tradeoff study for various PODs and repair qualities.

The ASIS and RPI can compute POF to the level of 1.e-20, even though there is no practical meaning when the POF is less than 1.e-8 or even 1.e-06. These values are presented for comparison purposes.

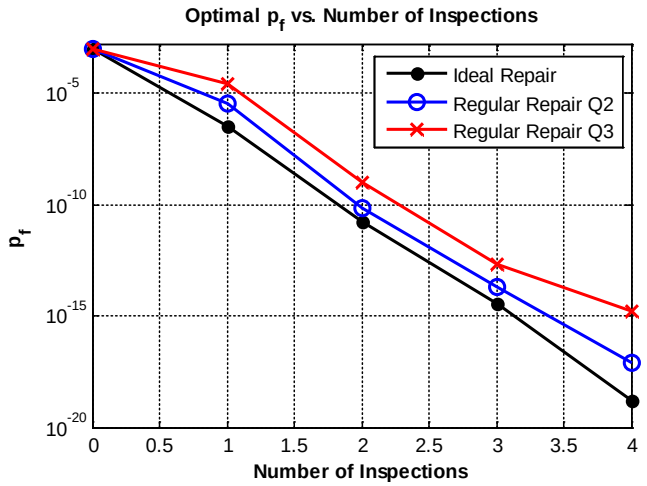

Figure 21. Comparison of the ideal and regular (Q3) repairs for 0 to 4 inspections

The optimal schedules for up to three inspections are summarized in figure 22. The following observations and explanations can be made:

1. The first-inspection time for the ideal repairs is approximately the same and exceeds half of the service life. The timing is strongly correlated with the earliest failures, as shown in figure 17 (i.e., the best first inspection time is just before the earliest failure [264,880 cycles] so that the POD is at the highest possible level before failures).
2. In all cases, the inspection schedules for the regular repairs are behind the schedules for the ideal repairs. This phenomenon can be traced to the fact that the Q2 and Q3 parts have shorter lives, and delaying the inspection time while risking more early failures can benefit by decreasing the p_f^W because of less ideal repaired parts. This explanation also implies that the delay time is correlated with the quality of the repair or, equivalently, the conditional p_f values. Therefore, the Q3 repair, which has a larger conditional p_f, can be expected to need more delays than Q2.

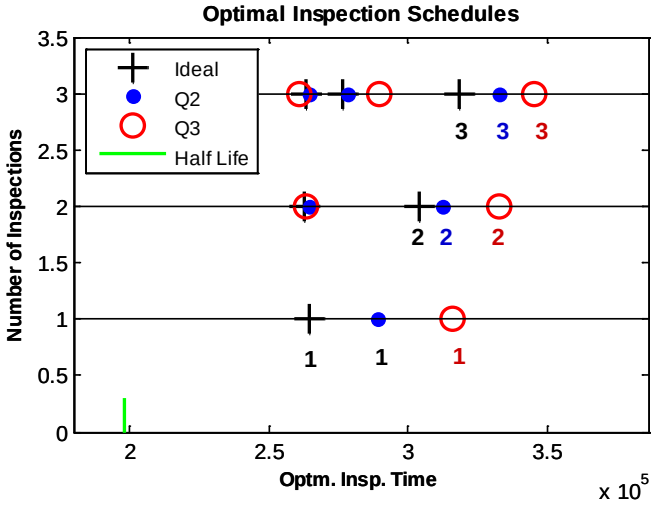

Figure 22. Optimal inspections for three repair qualities

2.3.7 Sensitivity Analysis Using Stage-1 Random Samples

Because there are uncertainties in the input assumptions, including initial defect size distribution, POD, and the calculated POF using limited stage 1 samples, the sensitivity of the selected optimal inspection schedules should be assessed. If the computed optimal point is highly sensitive, it may be necessary to settle for a suboptimal but more robust solution.

Figure 23 is a p_f scatter plot with 5000 randomly generated inspection plans for the ideal repair. The projections of the individual inspection points are shown in figure 24, which exploits the abrupt change of p_f around the first optimal inspection. The sudden increase of p_f is related to the earliest failures, meaning it would be too late if the early failures were not detected in time. Moreover, if more stage 1 failure samples were used in the RPI analysis, the time for the earliest failures, and therefore the first optimal inspection time, could be lower. Also, other input uncertainty may influence the p_f solution. Thus, the sensitivity plot suggests that, in practice, the first inspection time should be slightly smaller. The candidate for a robust solution can be found among the solutions that exceed the risk threshold.

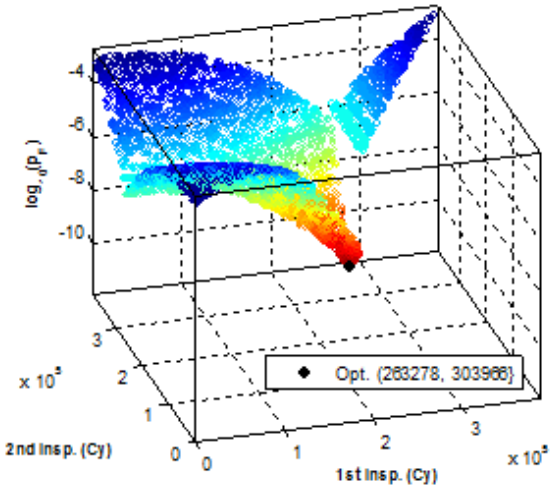

Figure 23. p_f for 5000 inspection plans (ideal repair with two inspections)

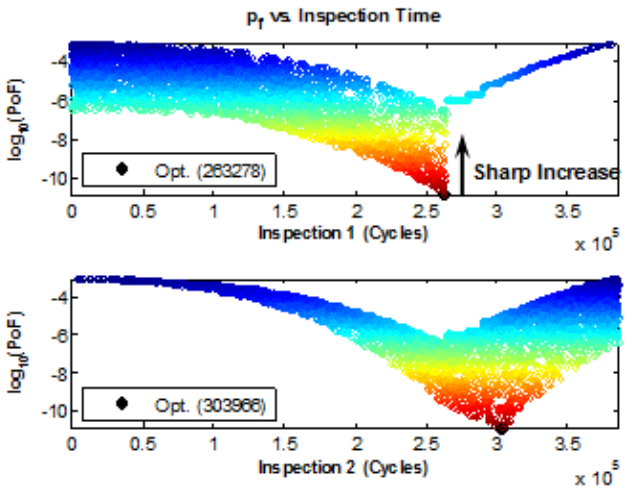

Figure 24. p_f vs. 5000 Inspection Plans (ideal repair with two inspections)

This approach for visualizing the sensitivity using random samples can be used for any number of inspections. Figure 25 shows the p_f function for three inspections for Q3 repair. The abrupt change of p_f around the first optimal inspection that appeared in the two-inspection case is also apparent. If desirable, more samples can be generated in the regions near the optimal points to more clearly assess the sensitivities and select better solutions.

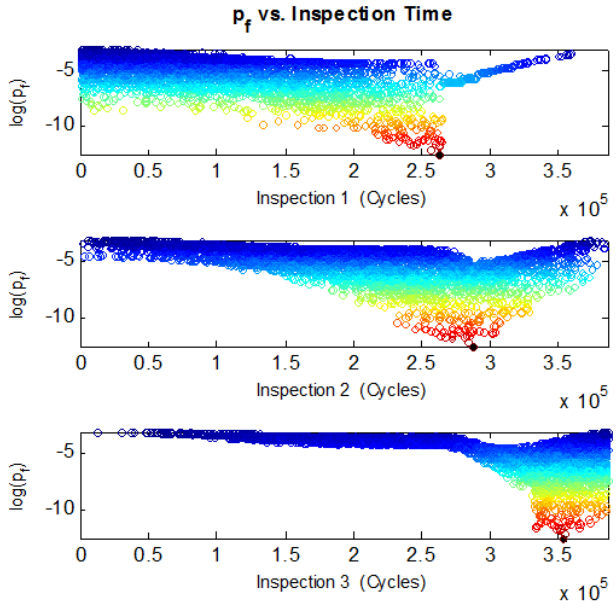

Figure 25. p_f vs. 5000 inspection plans (Q3 repair with three inspections)

2.3.8 Uncertain Probability of Detection

For problems in which the detection capability is highly uncertain, the effect of POD uncertainty can be assessed by a number of approaches, such as bounding or randomizing the parameters in

the POD function. In this study, we first used the nominal POD curve to identify the optimal inspection plan and then added RVs to the POD function to compute the distribution of POF. The result can be expressed by the probability-of-exceedance (POE) curve. From a decision-under-uncertainty perspective, the POE is related to risk and (1-POE) is the confidence. In practice, the decision is usually set at a high confidence, such as 90, 95, or 99%.

As an example, the mean and standard deviation of the nominal POD were both assigned a 20% coefficient of variation. Figure 26 shows the resulting POE curves for ideal and regular (Q3) repairs with two inspections. The range of p_f is very wide (approximately 1.e-05 to 1.e-20). At 90% confidence level, p_f is 1.3e-07, which is more than two orders of magnitude higher than the nominal value of 1.08e-09. This result suggests that the uncertainty of the POD is highly influential and a reduction of uncertainty may be beneficial.

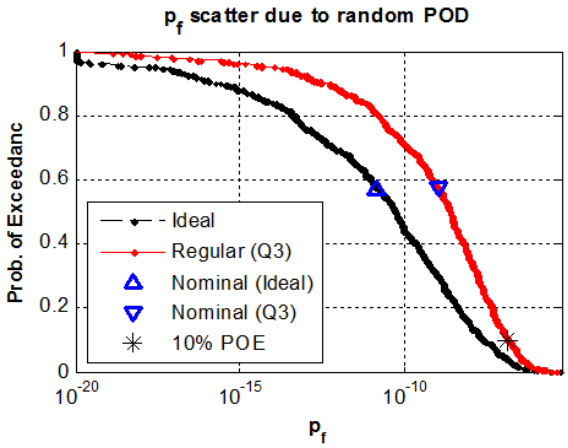

Figure 26. Probability-of-exceedance curves for ideal and Q3 repair

3. BAYESIAN UPATING METHDOLOGY

3.1 BAYESIAN FORMULATION

The prior distribution of an RV vector $\theta = [\theta_1, \theta_2, \ldots, \theta_J]$, $q^-(\theta)$ is updated to a posterior distribution, $q^+(\theta|D)$, by using N observed data, D, and a likelihood function, $L(D|\theta)$, which is written as:

$$q^+(\theta|D) = C \cdot L(D|\theta) \cdot q^-(\theta) \tag{8}$$

where C is the normalization factor:

$$C = \frac{1}{\int\cdots\int L(D|\theta)\cdot q^-(\theta)\cdot d\theta} \tag{9}$$

For DT applications, θ includes the statistical parameters (e.g., mean and standard deviations) of initial flaw size, POD, applied load, and fracture-mechanics modeling parameters. In general, the data D are the defect sizes determined during inspection from multiple locations and at multiple

points in time. The likelihood function is related to the PDFs of the defect sizes and the associated PODs.

Because smaller defects may be missed, the likelihood function should include both the detected and the missed likelihoods, and be defined using the product [28]:

$$L(\theta) = L_{Detected}(D_{Detected}|\theta) \cdot L_{Missed}(\theta) \tag{20}$$

in which the likelihood function for the detected defects is related to the PODs:

$$L_{Detected}(\theta) = \prod_{i=1}^{N_D} POD_i\left(D_i(t_i)\right) f(D_i(t_i)|\theta) \tag{21}$$

and the likelihood function for the non-detected defects is related to the PNDs:

$$L_{Missed}(\theta) = \prod_{i=1}^{N_{Missed}} \int PND_i\left(D(t_i)\right) \cdot f(D(t_i)|\theta) dD \tag{22}$$

The integral in equation 22 has the same value for the group of missed defects inspected at the same time and uses the same POD. In this case, equation 5 for the group becomes:

$$L_{Missed}(\theta) = \left[\int PND_i(D(t_i)) \cdot f(D(t_i)|\theta) dD\right]^{N_{Missed}} \tag{23}$$

To compute $L(\theta)$, the challenge is to compute the defect size PDF, $f(D(t_i)|\theta)$, for each defect that has been detected (either found or missed) at the associated time of detection, conditioned on each realization of θ. Moreover, because of the integral in equation 5, computing L_{Missed} requires $f(D(t_i)|\theta)$ for the entire range of $D(t_i)$.

Computationally, the crack size PDF for each detected size can be computed using a numerical differentiation scheme, that is:

$$f(D_i|\theta) = \lim_{\Delta\theta \to 0} \frac{\Delta F(D_i(t_i)|\theta)}{\Delta\theta} \tag{24}$$

where $F(D_i|\theta)$ is the CDF of the defect at D_i and can be computed by a reliability analysis method based on the following limit state formulation:

$$F_i(D_i|\,\theta\,) = \Pr[\mathrm{D}(X|\,\theta\,, t_i) < D_i] \tag{10}$$

where $D(X|\,\theta\,, t_i)$ is the defect size in the DT model. In the example below, the FPA software using the ASIS method was used to compute $F(D_i|\theta)$, but many other methods can be used [16-18].

The Bayesian update framework shown in figure 27 is based on the above derivations and the MCMC sampling approach. The updating process should be repeated whenever newer data are available.

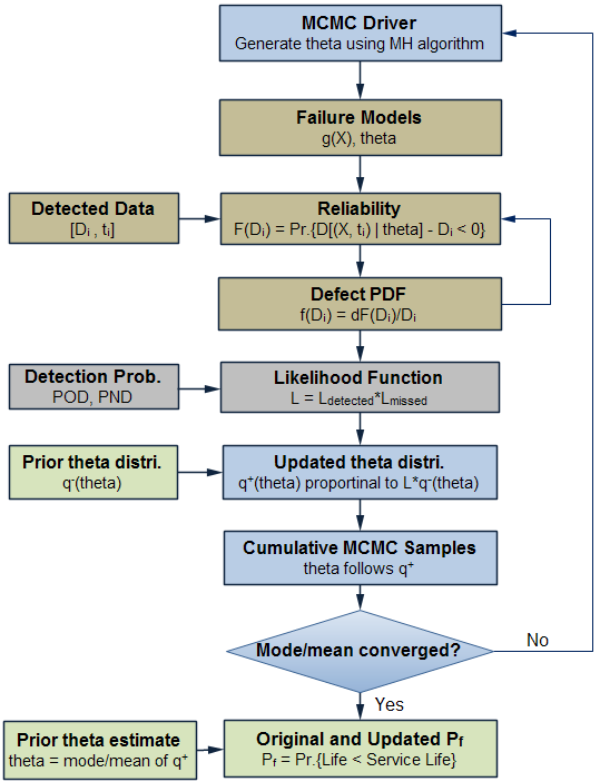

Figure 27. Bayesian-update flowchart for probabilistic DT

In this report, the MCMC samples are generated continuously until the mode (i.e., the most likely point) or the mean value of the posterior distribution has converged within a preset tolerance.

3.1.1 Develop Approximate Cumulative Distribution Function $F(D_i|\theta)$

The efficient computation of the likelihood function is critical to the performance of the above Bayesian updating. A response surface approach is proposed to overcome the computational challenge.

When using the simplest 2-point numerical scheme to estimate $F(D_i|\theta)$, the total number of times the CDF $F(D_i|\theta)$ needs to be calculated for $L_{Detected}$ is:

$$N(L_{Detected}) = 2 \cdot N_{Detected} \cdot N_{MCMC} \tag{11}$$

where N_{MCMC} is the number of MCMC samples required for updating θ. Assuming each point-CDF computation takes 5 CPU seconds using the a fast reliability method (more if using MC), and there are 10 detected defects, the total CPU time for generating 2000 MCMC samples would be 5*2*10*2000 = 200,000 seconds, or 55 hours. For L_{Missed}, the CPU time estimate is:

$$N(L_{Missed}) = 2 \cdot N_{Missed} \cdot N_{PDF} \cdot N_{MCMC} \tag{12}$$

where N_{PDF} is the number of CDF computations for computing the integral in equation 5 or equation 6. In general, the integral can be computed by taking the average of K samples as follows:

$$\begin{aligned} &\int PND\,(D_i) \cdot f(D_i|\theta) dD \\ &= E[PND(D_i)] = \frac{1}{K}\sum_{k=1}^{K}[PND(D_k)] \end{aligned} \tag{28}$$

An estimation could be made by assuming the MCMC algorithm is also used to generate crack-size samples and that 100 samples are sufficient to compute the average accurately. As such, the CPU time for one missed defect would be 5*2*100*2000 = 2,000,000 seconds, or 23 days. This would not be practical.

To overcome the computational issue, a response surface method has been developed to approximate the CDF of crack size as a function of θ and crack size. Assuming that 500 fitting points are needed, the CPU time required to compute the CDFs would be 5*(2*500) = 5,000 seconds, or 1.4 hours, which can be completed in a pre-processing mode. Parallel processing can be used in this mode.

The reason for creating the CDF rather than the PDF function is that CDF is a monotonic function that can be more easily fitted using regression or other response surface methods [23, 24, 29]. The response surface can be created before the MCMC loop or created on-demand during the MCMC process using a subset of the fitting points surrounding the sampled θ. With the response surface approach, the Bayesian update process should be significantly faster (e.g., in the order of minutes for 100 defects).

3.2 SAMPLING METHODS FOR BAYESIAN UPDATING

The MCMC method is widely used to generate posterior samples because of its unique ability to avoid the calculation of the normalization factor that is difficult for multiple dimensions [26, 27]. In this study, the Metropolis-Hastings algorithm was the preferred method for generating MCMC in the transformed, standardized normal space, u. By the nature of Markov Chain, the sequence of samples is correlated, and the quality of the random samples is inferior to MC. Consequently, a larger number of samples are usually needed to achieve convergence. In the example, 2000 samples were used to view the convergence, but, in general, a convergence criterion can be designed to adjust the number adaptively.

For reliability updating, the mode (i.e., the mostly likely point) of the posterior PDF may be suitable. In this case, a uniform sampling of θ can be used to identify the mode without regard to the shape of the posterior distribution. Parallel processing can be used in this option.

3.3 FRACTURE MECHANICS EXAMPLE

Though the methodology described above is intended for multiple detections at multiple times and includes both detected and missed defects, the example presented here is part of the initial testing of the proposed methodology and is limited to one inspection time with two unknown parameters. Also, to allow for validating the methodology in detail, the initial test assumes that the detection capability is very high at the time of inspection so that the chances of missing a defect can be ignored. The assumptions in this example will be removed in the future validation and development efforts.

The Bayesian software capability has been extended to analyze problems with multiple RVs. However, the current capability is limited to detected defects.

3.3.1 Analytical Model

The selected test problem is a fracture mechanics example involving random loading [29]. The limit-state function is:

$$g(t) = \int_{a_o}^{a_f} \frac{da}{\left(\varepsilon_Y Y(a)\sqrt{\pi a}\right)^m} - Cvt\varepsilon_S^m A^m \Gamma\left(1 + \frac{m}{B}\right) \tag{29}$$

where

a_o = Initial crack depth
a_f = Final crack depth at failure
$Y(a)$ = Geometry function of the crack shape
C, m = Crack growth parameter
v = Stress range annual frequency (cycles/year)
t = Time under consideration (year)
ε_Y = Model uncertainty for geometry
A, B = Weibull parameters for the long-term stress range distribution of $F_S(s) = 1 - e^{-(s/A)^B}$

The defect is a surface crack on a plate with a width of 10,000 mm and a thickness of 30 mm. The RVs and fixed parameters are listed in table 2.

From equation 29, the defect size as a function of time can be derived as:

$$a(t) = \frac{1}{\left[\frac{1}{\sqrt{a_o}} - \frac{Cvt\varepsilon_S^3 A^3 \Gamma\left(1 + \frac{3}{B}\right)}{2/\varepsilon_Y^3 (1.12)^3 \pi^{1.5}}\right]^2} \tag{30}$$

The POD has an exponential distribution with a mean value of λ:

$$POD(D) = 1 - \exp(-\lambda D) \tag{13}$$

Table 2. Input data for example

Name	Description	Distribution	Mean	Std. Dev.
ai	Initial crack depth (mm)	Exponential	0.11	0.11
C	Crack growth parameter (lnC)	Normal	-29.7	0.29997
ln_A	Weibull stress parameter (lnA)	Normal	2.26	0.14916
Inv_B	Weibull stress parameter (1/B)	Normal	1.43	0.1001
es	Stress modeling error	Normal	1	0.1
ey	Random geometry factor	Normal	1	0.1

Name	Description	Fixed Values		
vo	Average stress cycles per year	2.50E+06		
m	Crack growth parameter	3		
r	Cfack aspect ratio (a over C)	0.15		
z	Plate thickness (mm)	30		
b	Plate width (mm)	10000		
T	Time (years)	5		
af	Final crack depth (mm)	30		
am	Measured crack depth (mm)	10		

3.3.2 Modeling of θ

The exact initial flaw size has an exponential distribution with a mean value of 0.11 mm, which is the special case of Weibull with the same mean and standard deviation of 0.11 mm. Using the limit state of g = plate depth – $a(t)$, the p_f, computed using FPA, is 0.01225 at t = 10 years. The p_f was calculated by the ASIS method with a 5% error bound.

To test the performance of the Bayesian approach, two problems were considered. In problem 1, we assumed that the EIFS had an exponential distribution, but the mean value was uncertain and could only be estimated using a normal distribution with a mean value of 0.07 mm and a standard deviation of 0.015 mm. The estimated mean value 0.07 was 2.66 times the standard deviations away from the true mean. In problem 2, we assumed that the EIFS had a Weibull distribution with the mean of Normal (0.07, 0.015) and the standard deviation of Normal (0.13, 0.02). The estimated standard deviation was one standard deviation away from the true value. The objective of the testing was to see how well the Bayesian methodology could find the true values using 10 and 20 defects.

3.3.3 Simulation of Detection Data

To test the methodology, the defect sizes were simulated using the true initial flaw size. The selected time of inspection was t = 5 years. The defect sizes were randomly generated using equation 12. From a simulation, the first 20 defects were:

```
1.9512e-01  2.8870e-01  1.6843e-01  1.6901e-01  1.6282e-01
9.9993e-02  9.1542e-02  9.8584e-02  3.5774e-02  3.2228e-02
1.7613e-01  2.2200e-02  6.9054e-02  6.5349e-02  9.8356e-01
3.4708e-02  2.2806e-01  6.4161e-02  3.2253e+00  1.1542e-01
```

To focus the study on crack growth likelihood function issues, a large λ was intentionally selected so that all 20 defects were detected (i.e., there were no misses). Additional research is recommended to test a range of POD curves to create situations in which there are some misses, or only misses, to further test the above methodology.

3.3.4 Cumulative Distribution Function Response Surfaces

For each case, a response surface was created by computing the CDFs for 500 random sets of θ and a created by Latin Hypercube sampling. Second-order regression models were built. A sample is shown in figure 28, which proved to be satisfactory for the current example. Other meta-modeling methods [9, 16–18] most suitable for CDF approximation are being investigated for better accuracy and robustness.

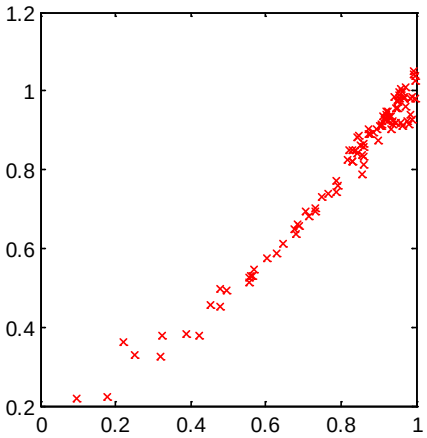

Figure 28. Example of regression model for crack CDF (exact vs. prediction)

3.3.5 Problem 1 With One Prior Variable

In both the 10 and 20 defect cases, 2000 MCMC samples were generated and the modes of the posterior PDFs were used to update the mean of the initial flaw size distribution and the p_f at 10 years.

For case 1 (10 defects), the prior p_f was 0.00807. In figure 29, the plotted posterior PDF was scaled using the ratio of the maximum PDFs for the prior and the posterior from the samples. It can be seen that the posterior PDF has shifted closely to the true value of 0.11. The history of the cumulative average of the posterior mean value is plotted in figure 30. After updating, the posterior p_f is 0.0108, which is closer to the true value of 0.01225.

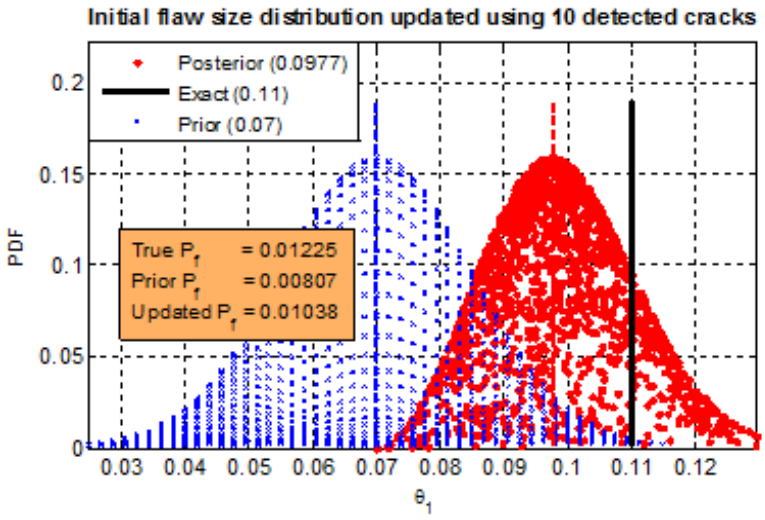

Figure 29. Problem 1 Bayesian updating (case 1: 10 detects)

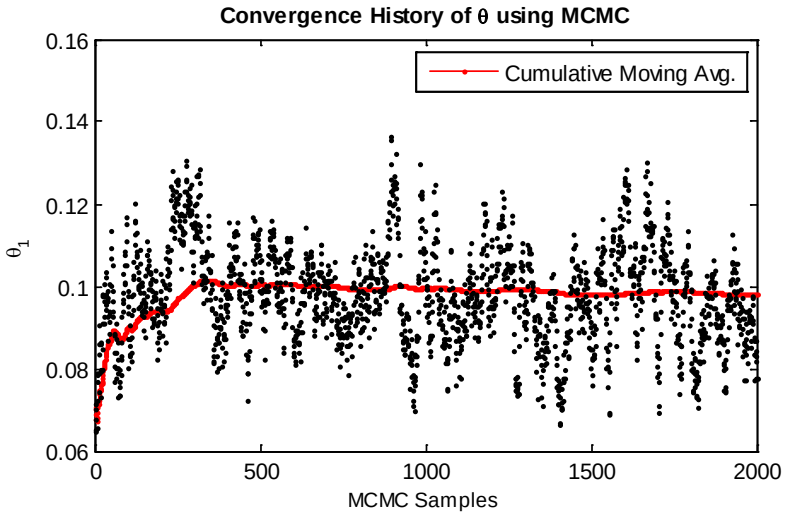

Figure 30. Convergence of MCMC for the posterior PDF (case 1: 10 detects)

For case 2 (20 defects), the scaled posterior PDF is plotted in figure 31. The posterior PDF has shifted much closer to the true value of 0.11. The history of the cumulative average of the posterior mean value is plotted in figure 32. After updating, the posterior p_f is 0.01231 (+/-5%), which is much closer to the true value of 0.01225 (+/-5%).

In summary, the updated PDF moved significantly closer to the true model using 10 defects. When 20 defects were used, the updated mode and the POF closely matched the true values.

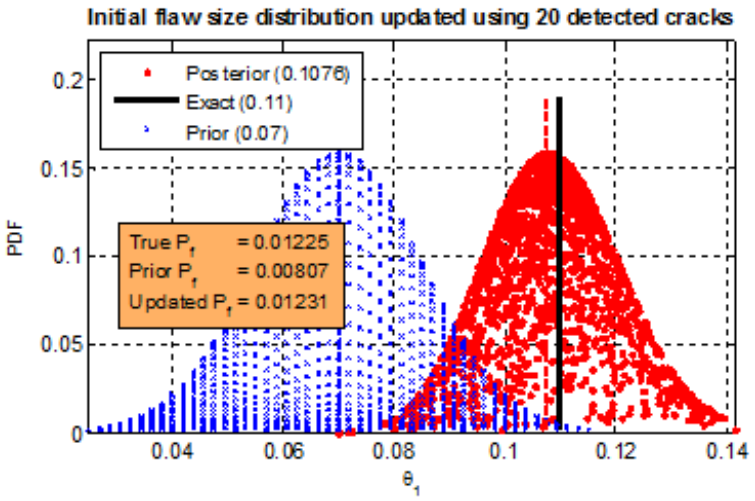

Figure 31. Problem 1 Bayesian updating (case 2: 20 detects)

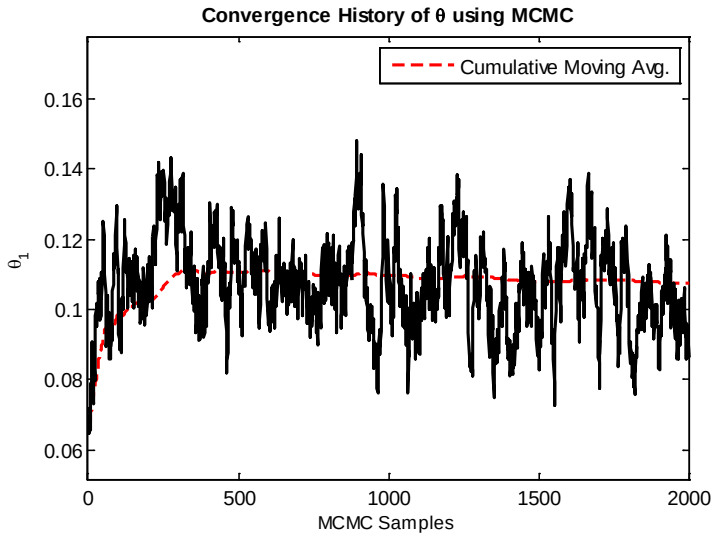

Figure 32. Convergence of MCMC for the posterior PDF (case 2: 20 detects)

3.3.6 Problem 2 With Two Prior Variables

In both the 10 and 20 defect cases, 2000 MCMC samples were generated, and the modes of the posterior PDFs were used to update the initial flaw size distribution and the p_f at 10 years.
For case 1 (10 defects), the prior p_f was 0.00881. The posterior PDF is plotted in figure 33. The history of the cumulative average of the posterior mean value is plotted in figure 34. After updating, the posterior p_f is 0.01079, which is closer to the true value of 0.01225.

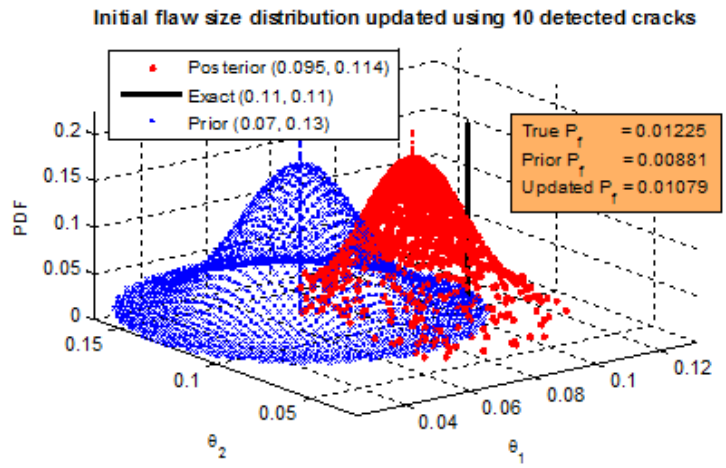

Figure 33. Problem 2 Bayesian updating (case 1: 10 detects)

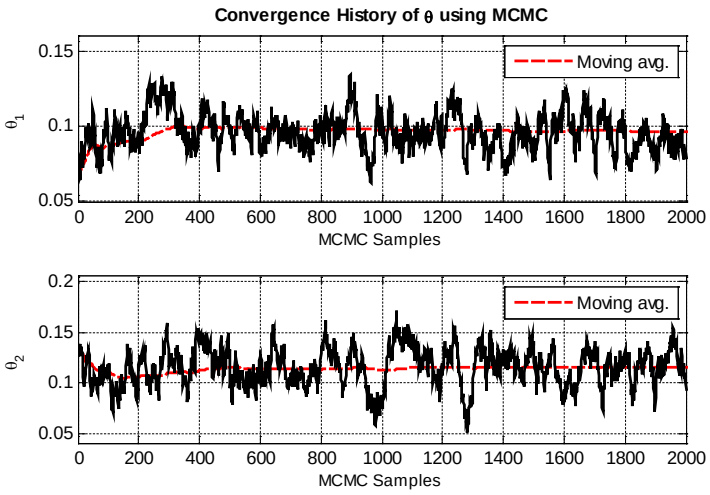

Figure 34. Convergence of MCMC for the posterior PDF (case 1: 10 detects)

For case 2 (20 defects), the scaled posterior PDF is plotted in figure 35. The posterior PDF has shifted much closer to the true value. The history of the cumulative average of the posterior mean value is plotted in figure 36. After updating, the posterior p_f is 0.0115 (+/-5%), which is closer to the true value of 0.01225 (+/-5%).

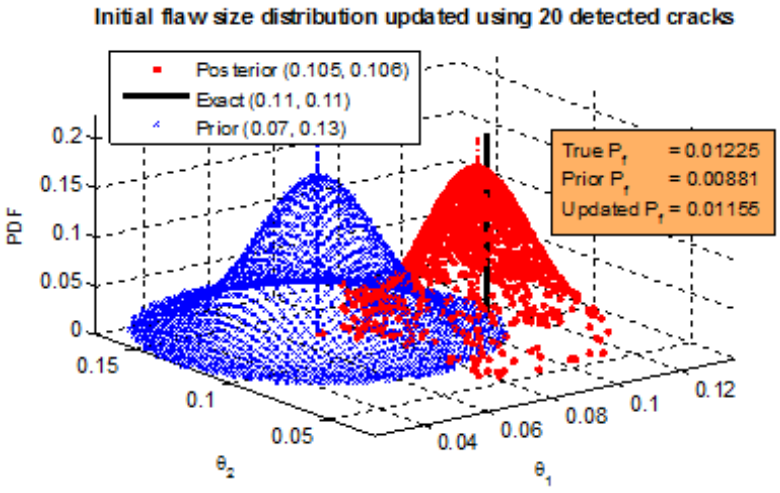

Figure 35. Problem 2 Bayesian updating (case 2: 20 detects)

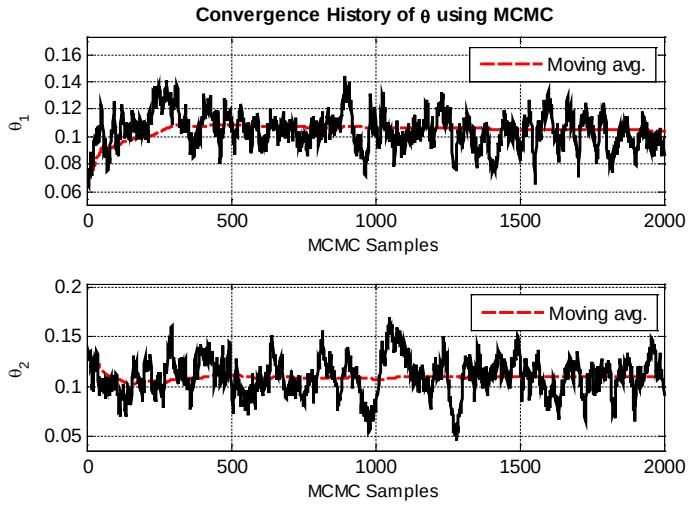

Figure 36. MCMC Samples for the posterior PDF (case 2: 20 detects)

In summary, the updated distribution moved significantly closer to the true model using 10 defects. When 20 defects were used, the updated mode and the POF matched the true values more closely. However, the match is not as good as in problem 1, possibly because that problem has only one prior variable, resulting in less uncertainty in the initial flaw size distribution.

4. SUMMARY AND DISCUSSIONS

An efficient RBMO methodology and software have been developed to facilitate the tradeoffs between the allowable risk, NDE devices (with associated POD), inspection schedules, and repair strategies. The methodology is built on a two-stage random simulation framework and three integrated methods: RAM, ASIS, and RPI. The methodology has been implemented in the FPA software and demonstrated using a DT application example involving the use of NASGRO

(Version 3.0) fracture mechanics code. The example included multiple RVs, a random POD, and several repair qualities with multiple inspections.

The FPA/RBMO analyses were carried out on a laptop computer with an Intel® Core™2 Duo processor @ 1.83 GHz. For the demonstration example, which represented a typical DT application, the total number of NASGRO executions for the original defect distribution included 63 runs for creating the RAM model and 1000 runs for generating the stage 1 failure samples. The RAM analysis portion, which included reliability analyses for updating the model, took 500 seconds. The additional 1000 NASGRO runs required 2700 seconds (approximately 2.7 seconds per sample), resulting in a total of 3200 seconds (53 minutes for stage 1 pre-processing). A similar amount of time was needed for each of the repair distributions. The number of MC samples equivalent to 1000 failure samples for the original defect distribution was 1.02 million, which would have required 45,000 minutes or approximately 31 days to generate. Thus, the total efficiency gain was more than 800 for the original defect distribution.

The saved crack growth data are repeatedly used in the stage 2 RPI analysis for any number of inspection plans. For the example, it took approximately 30 minutes for processing 5000 inspection plans for Ideal repair and 80 minutes for Q3 repair, both with three inspections. The analysis time for each repair case would have been multiplied by approximately three orders of magnitude if the standard MC method were used.

There are other meta-modeling methods that can be used. The uniqueness of the RAM approach is its ability to generate training data that matter the most to the accuracy of POF. The convergence of RAM is directly based on POF instead of the traditional goodness-of-fit of the model.

The foundation of the entire RBMO methodology is the two-stage framework that was built on the assumption that a safe structure would not be degraded because of maintenance. There is a possibility that a detected small and safe flaw can be repaired just like any other detected flaws. This risk is not treated in the current two-stage methodology and is a topic for additional investigation.

This report discusses the computational challenges and proposes an efficient computational strategy for updating probabilistic DT modeling assumptions using detection results from multiple inspections. The proposed strategy combines an efficient probabilistic DT methodology with MCMC to generate a posterior PDF and extract useful distribution parameters for subsequent reliability and maintenance updates.

A fracture mechanics example was developed to simulate the detected data to test the Bayesian update approach. The test case has demonstrated that the proposed computational strategy that integrates the MCMC and the response surface methods performed well. It is encouraging to note that even with the poor priors (one or more standard deviations away from the true value), the results have shown significantly improved posterior PDF using 10 defects and excellent improvement using 20 defects. Future work should investigate the effect of including missed defects and the relative merits from detected and missed data.

Though the presented methodology covers multiple detections at multiple times of detection, the example presented here, as part of the initial testing, is limited to one inspection. Nevertheless, the

simplified example has demonstrated the approach to generate time-dependent likelihood functions. Using the created CDF response surfaces, the 2000 MCMC samples could be completed in a few CPU minutes. Future examples will test more capabilities, including multiple inspection times, which will provide a transition to using SHM data.

For reliability updating, the mode (i.e., the most likely point) of the posterior PDF may be suitable. In this case, a uniform sampling of θ can be used to identify the mode without regarding the shape of the posterior distribution. This approach should be investigated because parallel processing can be used to improve the computational speed.

5. REFERENCES

1. Shiao, M., "Risk-Based Maintenance Optimization," in *Proceedings of the International Conference on Structural Safety and Reliability,* (ICOSSAR), pp. 3231–3237, Rome, Italy, June 19–23, 2005

2. Wu, Y-T., Shiao, M., Shin, Y., and Stroud, W.J., "Reliability-Based Damage Tolerance Methodology for Rotorcraft Structures," *Transactions Journal of Materials and Manufacturing*, paper 2004-01-0681, July 2005.

3. Wu, Y-T., Zhao, J., Shiao, M., and Millwater H.R. "Efficient Methods for Probabilistic Damage Tolerance Inspection Optimization," *Proceedings of the 51st AIAA/ASME/ASCE/AHS Structures, Structural Dynamics and Materials Conference*, Orlando, Florida, April 2010.

4. Ang, A. H.-S and Tang, W.H., *Probability Concepts in Engineering Planning and Design, Volume II; Decision, Risk, and Reliability*, John Wiley & Sons, New York, 1984.

5. Harris, D.O., "Probabilistic Fracture Mechanics, Probabilistic Structural Mechanics Handbook Theory and Industrial Applications," (C. Sundararajan, ed.) Chapman & Hall, New York, 1995, Ch. 6, pp. 106-145.

6. Shiao, M., "Risk Forecasting and Updating for Damage Accumulation Processes with Inspections and Maintenance," *5th International Workshop on Structural Health Monitoring*, Stanford, California, September, 2005.

7. Ellingwood, B., "General-Purpose Software for Structural Reliability Analysis," *Structural Safety*, Vol. 28, No. 1 and No. 2, January–April 2006.

8. Wu, Y.-T. Shin, Y., Sues, R., and Cesare, M., "Probabilistic Function Evaluation System (ProFES) for Reliability-Based Design," *Journal of Structural Safety*, Vol. 28, No. 1 and No. 2, January–April 2006, pp. 164–195.

9. Wu, Y-T., Shiao, M., Zhao, J., and Millwater, H.R., "Recent Advances in Methods and Software for Probabilistic Damage Tolerance Inspection Optimization," Presented at *AHS Meeting on Rotorcraft Structures and Survivability*, Williamsburg, VA., Oct. 27–29, 2009.

10. Thoft-Christensen P., and Murotsu, Y., *Application of Structural Systems Theory*, Springer, 1986.

11. Melchers, R.E., *Structural Reliability: Analysis and Prediction*, John Wiley & Sons, 1987.

12. Wu, Y.-T., Millwater, H.R., and Cruse, T.A., "An Advanced Probabilistic Structural Analysis Method for Implicit Performance Functions," *AIAA Journal*, Vol. 28, No. 9, 1990 pp. 1663–1669.

13. Ditlevsen, O. and Madsen, H.O., *Structural Reliability Methods*, John Wiley & Sons, New York, 1996, pp.384.

14. Schueller, G.I., "Structural Reliability—Recent Advances," *Proc. 7th ICOSSAR'97*, Kyoto, Japan, 1998, pp. 3–33.

15. Au, S.K. and Beck, J.L., "Estimation of Small Failure Probabilities in High Dimensions by Subset Simulation," *Probabilistic Engineering Mechanics*, Vol. 16, No. 4, 2001, pp. 263–277.

16. Rackwitz, R., "Reliability Analysis—A Review and Some Perspectives," *Structural Safety*, Vol. 23, 2001, pp. 365–395.

17. Der Kiureghian, A., "First- and Second-Order Reliability Methods," Chapter 14 in *Engineering Design Reliability Handbook*, Nikolaidis, E., Ghiocel, D. M., and Singhal, S., Eds., CRC Press, 2005.

18. Nikolaidis, E., Ghiocel, D.M., and Singhal, S., eds, *Engineering Design Reliability Handbook*, CRC Press, Boca Raton, Florida, 2005

19. Wu, Y-T., Enright, M.P., and Millwater, H.R., "Probabilistic Methods for Design Assessment of Reliability With Inspection," *AIAA Journal*, Vol. 40, No. 5, 2002, pp. 937–946.

20. Wu, Y-T. and Shin, Y, "Probabilistic Damage Tolerance Methodology for Reliability Design and Inspection Optimization," *Proceedings of the 45th AIAA/ASME/ASCE/AHS Structures, Structural Dynamics and Materials Conference*, Palm Springs, California, April 19–22, 2004.

21. Wu, Y.-T. and Shiao, M., "Sampling-Based Fast Probability Analyzer for Reliability-Based Maintenance Optimization," *Proceedings of the International Conferences on Structural Safety and Reliability* (*ICOSSAR '09*), ASCE, Osaka, Japan, September 12–17, 2009.

22. Zacks, J., Schiller, S.B., and Welch, W.J., "Design for Computer Experiments," *Technometrics*, Vol. 31, No. 1., 1989.

23. Fang, K-T., Li, R., and Sudijanto, A., “Design and Modeling for Computer Experiments,” Chapman and Hall/CRC, 2006.

24. Hardle, W., Muller, M., Sperlich, S., and Werwatz, A., *Nonparametric and Semiparametric Models*, Springer-Verlag, 2000.

25. Gamerman, D., *Markov Chain Monte Carlo*, Chapman and Hall, 1997.

26. Robert, C.P., and Casella, G., *Monte Carlo Statistical Methods*, Springer, 2004.

27. Ang, G.L., Ang, A.H-S., and Tang, W.H., “Optimal Importance Sampling Density Estimator,” *Journal of Engineering Mechanics*, Vol. 118, No. 6, June 1992, pp. 1146–1163.

28. Hovey, P.W., Berens, A.P., and Knopp, J. “Estimating the Distribution of the Size of Flaws Remaining After an Inspection”, AFRL-ML-WP-TP-2006-496.

29. Ku, A., Serratella, C., Spong, R., Basu, R., Wang, G., and Angevine, D., “Structural Reliability Applications in Developing Risk-Based Inspection Plans for a Floating Production Installation,” OMAE 2004-51119, 2004.